Comparative population genomics unveils congruent secondary suture zone in Southwest Pacific Hydrothermal Vents

AUTHORS :

Adrien Tran Lu Y[1,3]*, Stéphanie Ruault[2], Claire Daguin-Thiébaut[2], Anne-Sophie Le Port[2], Marion Ballenghien[2], Jade Castel[2], Pierre-Alexandre Gagnaire[1], Nicolas Bierne[1], Sophie Arnaud-Haond[3], Camille Poitrimol[2], Eric Thiébaut[2], François H Lallier[2], Thomas Broquet[2], Didier Jollivet[2], François Bonhomme[1] & Stéphane Hourdez[4]

Affiliations :

1 : ISEM, Univ Montpellier, CNRS, IRD, Montpellier, France

2 : Sorbonne Université, CNRS, Station Biologique de Roscoff, UMR 7144 Adaptation and diversity in the marine environment, Place Georges Teissier, 29 680 Roscoff, France

3 : MARBEC UMR 248, Université de Montpellier, Ifremer, IRD, CNRS; Avenue Jean Monnet CS 30171, 34203, Sète, France

4 : UMR 8222 LECOB CNRS-Sorbonne Université, Observatoire Océanologique de Banyuls, Avenue du Fontaulé, 66650, Banyuls-sur-mer, France

*Corresponding author : dr.adrien.tranluy@gmail.com

Abstract

How the interplay of biotic and abiotic factors shapes current genetic diversity at the community level remains an open question, particularly in the deep sea. Comparative phylogeography of multiple species can reveal the influence of past climatic events, geographic barriers, and species life history traits on spatial patterns of genetic structure across lineages.

Here, we conducted a comparative population genomic study on seven hydrothermal vent species co-distributed in the Back-arc Basins of the Southwest Pacific region. Using ddRAD-seq, we compared distribution range-wide genomic diversity patterns across species and discovered a shared zone of phylogeographic break. Although species exhibit congruent patterns of spatial structure, they also show variation in the degree of divergence among lineages across the suture zone. Additionally, two species have a sympatric contact zone in the Woodlark Basin.

Demogenetic inference revealed shared histories of lineage divergence and secondary contact. Low levels of asymmetric gene flow probably occurred in most species between the Woodlark and North Fiji basins, but the exact location of contact zones varied from species to species. Results show that gene flow is heterogeneous across the genome, indicating possible partial reproductive isolation between lineages and early speciation.

Our comparative study sheds light on the factors that shape genetic variation at the community level, and our findings enrich our understanding of deep-sea biogeography patterns. Emphasizing the pivotal role of historical and contemporary factors, our research underscores the necessity for a holistic approach, and in particular filling in the gaps regarding life history traits of deep-sea species (generation time, development type, duration of the larval phase).

Introduction

Hydrothermal vents are one of the most emblematic chemosynthesis-based ecosystems that host a highly specialized fauna. This vent fauna depends on local hydrothermal activity and is likely to share historical patterns of colonization linked to the tectonic history of the ridge system (Plouviez et al., 2009, Matabos et al., 2011, Matabos & Jollivet., 2019). In contrast to other deep-sea ecosystems, vents represent a linear but highly fragmented and relatively unstable ecosystem based on chemosynthetic primary producers, which cannot thrive elsewhere. Hydrothermal activity is linked to specific geological features associated with the volcanic and tectonic activities of ocean ridges or submarine volcanoes (Hourdez and Jollivet, 2020). Plate tectonics has previously been cited as a driver of most of the biogeographic distribution of the vent fauna (Tunnicliffe, 1991), that may lead to allopatric speciation with possible secondary contacts (Hurtado et al. 2004, Johnson et al. 2006, 2013, Faure et al. 2009, Plouviez et al., 2009, Matabos et al. 2011). On the East Pacific Rise, these previous studies pointed toward the emergence of a transition zone between biogeographic provinces initially separated.

Unlike other hydrothermal ecosystems, the fauna of the vents of the South-West Pacific is distributed across several geological Back-Arc-Basins (BABs) separated by abyssal plains, ridges and volcanic arcs, forming a fragmented and discontinuous complex. These BABs formations are estimated to be between 12 to 1 million years (My) old (Schellart et al., 2006). A Previous study highlighted contrasting phylogeographic patterns for few species, including some closely related species (Poitrimol et al., 2022). This suggested alternative dispersal strategies and evolutionary history to cope with fragmentation despite a common geological history of the vent habitat in this region. This geological dynamics provided a completely different and discontinuous situation of hydrothermal environments, in sharp contrast to the linear setting of mid-oceanic ridges such as the Mid-Atlantic Ridge (MAR) or the East Pacific Rise (EPR). These unique features raise questions about how abiotic and biotic factors shape the distribution of genetic diversity and the connectivity between populations of different lineages.

The vent fauna and communities inhabiting these Southwest Pacific BABs appear as a single biogeographic unit (Bachraty et al., 2009; Moalic et al., 2012; Tunnicliffe et al., 2024). In contrast to other hydrothermal communities, which are mainly composed of tubeworms,

mussels and shrimps, the BAB fauna is mainly composed of large symbiotic Provannidae gastropods, such as *Ifremeria nautilei* or *Alviniconcha spp*., and deep-sea *Bathymodiolus* mussels. These large engineer species create specific habitats for a wide assemblage of invertebrate species, including annelids from different families (e.g. Polynoidae, Alvinellidae, Siboglinidae), limpets (*Lepetodrilus* spp., *Shinkailepas* spp.), barnacles, holothurians, and crustaceans (copepods, amphipods, shrimps, and crabs) (Desbruyères et al., 2006).

While these vents form thriving oases of life, they also produce metallic sulfide deposits, which attract the interest of deep-sea mining companies. The upcoming management of the Southwest Pacific vent fauna will rely on understanding population delimitation and parameters, which are of crucial importance in conservation biology (Gena, 2013; Niner et al., 2018; Van Dover, 2011; Van Dover et al., 2017; Washburn et al., 2019). Anthropogenic exploitation of vent resources has already begun on a Japanese site in the Northwest Pacific and has been first planned in the Manus BAB (Solwara prospects) but recently abandoned, although the potential consequences of these activities are not yet known (Carver et al., 2020).

Connectivity and renewal of vent populations is mostly driven by larval dispersal due to the sedentary nature and the strict relationship with the vent fluid. While some vagile fauna, such as fish, crabs, or shrimp, may contribute to connectivity through adult migration in response to local environmental changes, but only to very limited spatial scale (vent fields) (Lutz et al., 1994; Shank et al., 1998). Direct connectivity assessment is not technically feasible for minute larvae numbering in millions and their life-traits characteristics (Levin, 1990, Vrijenhoek, 2010). As consequence, demographic connectivity needs to be assessed by indirect methods such as population genetics, larval dispersal modeling or recent method of elemental fingerprints tracking (Mouchi et al. 2024).

Dispersal modeling in the region suggested possible but limited larval exchange between distant back-arc basins (Mitarai et al., 2016). However, in the context of the unstable and fragmented habitat of deep-sea hydrothermal vents, metapopulation theory predicts long-distance dispersal to mitigate risks of inbreeding and local extinction (Hamilton & May, 1977; McPeek & Holt, 1992). Initial genetic analyses of several vent species along mid-oceanic ridges however displayed conflicting evidence regarding dispersal capabilities, with some suggesting almost panmictic populations at the ridge scale while others hint at patterns of isolation by distance and stepwise (re)colonization (Teixeira et al., 2012; Audzijonyte & Vrijenhoek, 2011).

Present-day geographical distribution of genetic diversity reflects the complex interplay of connectivity patterns across space and time. Studying and disentangling the origin of these variations is the main objective of phylogeography (Avise, 2000, 2009; Avise et al., 1987). Expanding this approach, to a multispecies comparative framework within a given biome or ecosystems can highlight the effect of several factors shaping the genetic diversity (Hickerson et al., 2010; Papadopoulou & Knowles, 2016). Using new methods and approaches for large genomic dataset, we can start to disentangle past and present connectivity patterns and offer a unique opportunity to describe species distribution patterns at the community level and to improve scientific guidelines for conservation (De Jode et al., 2023, Gagnaire, 2020).

Our study aimed to elucidate genetic diversity and connectivity patterns across a biogeographic hydrothermal unit in the South West Pacific. We conducted a comparative population genomics analysis on seven vent species spanning various taxonomic groups inhabiting the same environment and geographic range, covering most basins of the South West Pacific region. Phylogeographic patterns exhibited by these species, each characterized by distinct life-history traits, were compared at a regional scale using a genome-wide analysis. This analysis revealed a clear phylogeographic break encompassing all seven species around the Solomon-Vanuatu archipelago islands, alongside a contact zone on the Woodlark ridge observed in two species. Based on inferred demogenetic histories, we propose a scenario of vicariance for all species. Furthermore, estimating genetic diversity and gene flow at the community scale underscores the importance of comprehending population connectivity across different geographic scales. This understanding is vital for informing potential management strategies, particularly in the context of future deep-sea mining activities, and for gaining more insights into biogeography of deep-sea species.

142 ## Material and methods

143 ***Sampling***

144 Seven hydrothermal-vent species from four main vent habitats have been sampled over five
145 Western Pacific regions (the Manus, Woodlark, North Fiji, Lau back-arc basins) and the Futuna
146 volcanic arc (see SI Table 1 and Figure 1). These species include the emblematic symbiotic
147 snails *Ifremeria nautilei* and *Alviniconcha kojimai*, the vent mussel *Bathymodiolus manusensis*,
148 the limpets *Shinkailepas tollmanni*, *Lepetodrilus schrolli*, and *L. aff. schrolli* (recently described
149 as *L. fijiensis* by Chen & Sigwart 2023 in North Fiji, Lau and Futuna BAB), which live on the
150 shells of *I. nautilei, Bathymodiolus manusensis* and *B. septemdierum,* the cirriped
151 *Eochionelasmus ohtai*, mostly found on the edge of diffuse venting areas, and, finally, the large
152 scaleworm *Branchinotogluma segonzaci*, found on the walls of vent chimneys. Animal
153 collections were made during the Chubacarc cruise in 2019 (chief scientists S. Hourdez & D.
154 Jollivet) on board the RV *L'Atalante* with the ROV Victor 6000 (Hourdez & Jollivet 2019). All
155 species, with the exception of *B. segonzaci,* were sampled from diffuse venting areas with the
156 tele-manipulated arm of the ROV and brought back to the surface in thermally insulated
157 boxes. The mobile chimney scaleworms *B. segonzaci* were collected using the slurp gun of the
158 ROV and kept in 5 L bottles until the ROV recovery. On board, large animals (provannid
159 gastropods, mussels, cirripedes and scaleworms) were dissected to separate tissues and
160 individually preserved in 80% ethanol, and/or directly used for DNA extractions. A hierarchical
161 sampling scheme was used for all species by sampling two replicate sites within each vent field
162 (locality) and one to three vent fields per basin, for a total number of 21 sampling localities
163 for each vent community (SI Table 1). A total number of 24 individuals were preserved for DNA
164 extraction (or extracted directly) for each locality replicate and species.

165 This sampling scheme was however not possible for *B. manusensis*. It was only found at
166 Manus, Futuna and one site of Lau (at the Mangatolo locality) in sympatry with *Bathymodiolus*
167 *septemdierum* (previously known as *B. brevior*). It was not found at the site La Scala in the
168 Woodlark Basin (no mussels), nor at the Southern localities of the Lau Basin and along the
169 North Fiji Ridge, where *B. septemdierum* was only found. DNA extractions were directly
170 performed on board for *I. nautilei* (foot tissue), *A. kojimai* (foot tissue), *B. manusensis* (mantle
171 tissue), *S. tollmanni* and *L. schrolli & L. aff schrolli (now L. fijiensis)* (whole individual without
172 the shell) and *E. ohtai* (whole individuals without the skeleton). For *B. segonzaci,* DNA

extractions were done later in the laboratory on ethanol-preserved tissues. DNA extractions were either performed with a modified CTAB 2%/PVPP 2% protocol (see Jolly et al. 2003) or the NucleoSpin®Tissue 96 kit (Macherey-Nagel, Karlsruhe, Germany).

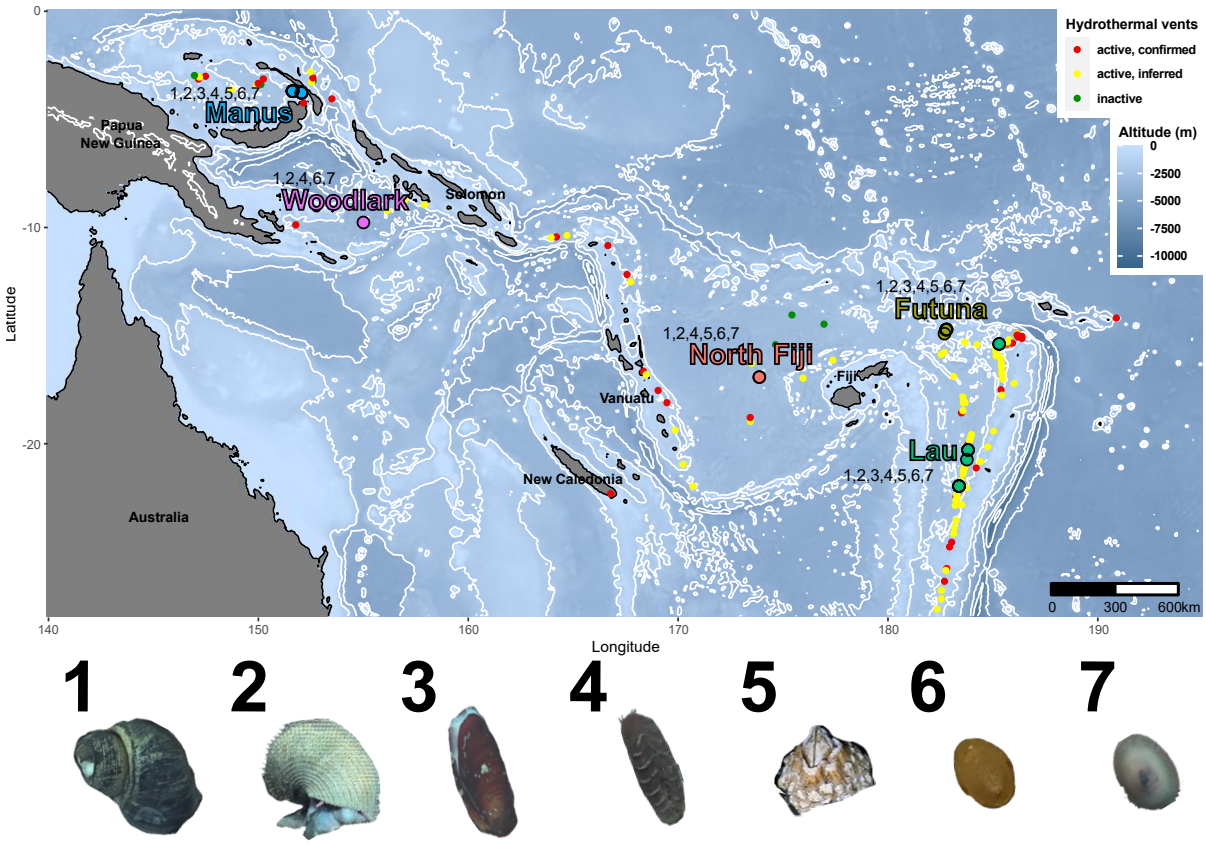

Figure 1: Sampling areas in the South-west Pacific Ocean. Colors represent the different areas (BABs and volcanic arc). Each square box contains species found and sampled for each sampling area. 1: I.nautilei, 2: A. kojimai, 3: B. manusensis 4: B. segonzaci, 5: E. ohtai, 6: S. tollmanni and 7: L. schrolli (& fijiensis). Small points represent hydrothermal vents. Red, active and confirmed. Yellow, Active and inferred. Green, Inactive. Vents activity data taken from InterRidge Vents Database V3.4.

Preparation of the ddRAD Libraries.

The preparation of ddRAD genomic libraries was standardized by following the protocol described in Daguin-Thiébaut et al. (2021) and used for *I. nautilei* in Tran Lu Y et al. (2022). These seven libraries comprise 294 individuals for *A. kojimai* (from Castel et al. (2022)), 469 individuals for *S. tollmanni*, 282 individuals for *E. ohtai*, 195 individuals for *B. manusensis*, 262 individuals for *B. segonzaci*, and 522 individuals for *L. schrolli & L. fijiensis*. All libraries were produced from gDNA digested with the enzymes *Pst1* and *Mse1,* except for *B. manusensis* that was digested with *Pst1* and *Msp1*.

190 These libraries also included 8 to 47 replicates (individuals replicated twice or three times as
191 controls) used for quality control and parameter calibration. Single-end (only for *B.*
192 *manusensis*) or paired-end 150 sequencing (all other taxa) was performed on HiSeq 4000 (*I.*
193 *nautilei*) or Novaseq 6000 Illumina (all other taxa), by the Genoscope, France (*I. nautilei*), or
194 Novogene Europe (Cambridge, UK; all other taxa). The Fastqc Software (V.0.1.19) was used to
195 check the sequence quality of the raw reads prior to the *de novo* assembly for each species.

196 An independent assembly was performed from each species library with the "*de novo"* Stacks2
197 module (Rochette et al., 2019) after demultiplexing individuals with the Process_radtags
198 module. Parameter calibration approach followed the recommendations of Mastretta-Yanes
199 et al. (2015) and Paris et al. (2017), (see SI Calibration). For all species, the parameter
200 calibration approach, data filtering, and the Stacks modules used were consistent with the
201 methods described in Tran Lu Y et al. (2022). However, for *S. tollmanni* and *L. schrolli* & *L.*
202 *fijiensis*, the data filtering was slightly modified to reduce the loss of SNPs and individuals while
203 minimizing the proportion of missing data due to a greater allele divergence (SI Table 2).
204 Additionally, for each species, the minor allele frequency filter was replaced by a masking of
205 singletons in the demogenetic inference datasets (i.e. used with ðaði). Finally, the "*de novo*"
206 assembly of *B. manusensis* data was realized from single-end reads (R1, 150 bp).

207 ***Population structure and admixture across the southwest Pacific***

208 For each species, a series of independent population genomics analyses were performed to
209 explore the population structure, phylogeographic and admixture patterns. Principal
210 Component Analysis (PCA) was performed on individual genotypes with SNPRelate (V.1.21.7)
211 to explore the spatial distribution of genetic diversity (Zheng et al., 2012). Further analyses to
212 explore population differentiation and admixture proportions were performed with the
213 software Admixture (V.1.3.0) (Alexander & Lange, 2011). Population trees including migration
214 edges and F_3 statistics were computed with the software Treemix (V.1.13) (Pickrell & Pritchard,
215 2012) with ten replicates and migration events from 0 to 5.

216 The degree of genetic differentiation was estimated with pairwise F_{st} values between groups
217 of individuals (genetic units or metapopulations, basins or localities) with Arlequin (V.3.5.2.2)
218 (Excoffier & Lischer, 2010) and their statistical significance was assessed with 10,000
219 permutations of genotypes between populations. All plots were produced with R (V.4.0.3) (R

220 Core Team, 2023) and ggplot2 (V.3.3.6) (Wickham, 2016). For *S. tollmanni,* Woodlark
221 individuals were split into two groups according to their genetic assignment (See results).

222 In addition, the net divergence between two populations (D_a) was calculated from the
223 measure of absolute divergence (D_{xy}) corrected by the average nucleotide diversity (π)
224 estimated using Stacks2 (Rochette et al., 2019) by following the formula of Nei & Li (1979).
225 The genetic diversity indices (*He*, *Ho*, π) were also calculated for each species with the Stacks
226 (V.2.52) population module on the final dataset. Indices were estimated for each genetic unit
227 found by PCA and the Admixture analysis, which number depends on the species considered
228 and on geography (five geographic regions/BABs listed in SI Table 1).

229 ***Evolutionary history of vent species and metapopulation connectivity***

230 **Relative gene flow orientation.**

231 Gene flow orientation was assessed with the module Divmigrate (Sundqvist et al., 2016)
232 contained in the R package diveRsity (V.1.9.90) (Keenan et al., 2013). This method uses allele
233 frequencies and several estimators derived from the Fst statistics to calculate a migration
234 matrix between populations, which is then normalized by the highest gene flow value found
235 in the pairwise comparisons, setting gene flow value between 0 and 1 (where 1 represents
236 100% gene flow and 0, no gene flow). Statistical significance of the difference between gene
237 flow directions in a given pair of populations was estimated with 1000 bootstraps.

238 **Demogenetic history of species metapopulations**

239 To understand the demographic history of populations and identify the best model of
240 population divergence, we fitted joint allele frequency spectra to specific population models
241 with the *∂a∂i* software (V2.1.0) (Gutenkunst et al., 2009) for each taxon independently,
242 considering the case of an ancestral population splitting into two daughter populations with
243 or without migration. Our choice was dictated by the fact that populations of all vent species
244 analyzed (with the exception of *L. schrolli & L. fijiensis*, see results) are only subdivided into
245 two genetic units (Eastern vs. Western populations). Although, *L. schrolli & L. fijiensis* displays
246 further minor subdivisions between basins, for the sake of the comparison with other species,
247 we considered Eastern (NF/L) vs Western populations (M) (see discussion). One of the main
248 advantages of the *∂a∂i* approach is that it takes into consideration the effects of linked
249 selection and heterogeneous migration across the genome. Ignoring these effects in

250 demographic inference may lead to erroneous reconstructions of the evolutionary history of
251 populations (Ewing & Jensen, 2016; Ravinet et al., 2017). To discuss patterns of divergence
252 and past and present genetic connectivity of all species, we re-used the models implemented
253 in Tran Lu Y et al. (2022) with a similar population design for all taxa. These models considered
254 a total of 28 possible scenarios extended from the 4 major divergence models (Strict Isolation
255 (SI), Isolation with Migration (IM), Ancient Migration (AM) and Secondary Contact (SC)) that
256 were initially developed and used in Rougeux et al. (2017) (also see Tran Lu Y et al., 2022 for
257 further details). Briefly, different demographic and evolutionary processes have been
258 considered within these models, such as the increase or the contraction in size of the two
259 derived populations (G), the effect of barrier loci due to either hybrid counterselection or local
260 adaptation by simulating heterogeneous migration along the genome (2m) and the effect of
261 linked selection (2N).

262 The ancestral allele of each locus could not be identified because no external groups were
263 available (or too divergent) for any of the taxa. Hence, we used folded joint allele frequency
264 spectra (folded JAFS). All models were fitted 10 times independently for each species to check
265 for model convergence. The Akaike Information Criterion (AIC) was used to compare models
266 for each simulation. Given the gaps in the knowledge of the biology of these taxa, we
267 estimated model parameters and divergence times (i.e. Ts since divergence, Tsc since
268 secondary contact, and the absolute divergence time, which can be Ts or Ts+Tsc) using an
269 average mutation rate of 10^{-8}. Parameter uncertainties were calculated using the Fisher
270 Information Matrix (FIM) on the best fit model for each species. The uncertainties are
271 calculated at the 95% confidence level.

272 **Results**

273 ***Calibration parameters and filtering steps.***

274 The 150 bp paired-end sequencing yielded an average of 3.7, 3.3, 3.0 and 2.8 million of paired
275 reads per individual for *S. tollmanni*, E. *ohtai, B. segonzaci* and *L. schrolli & L fijiensis*,
276 respectively. For *B. manusensis,* single read data were obtained with 2.9 million reads per
277 individual. The raw reads used from *A. kojimai* and *I. nautilei* were obtained following the
278 protocol described in Castel et al. (2022) and Tran Lu Y et al. (2022).

279 For each species, we identified the most appropriate set of assembly parameters with Stacks
280 (V.2.52) by applying the same pipeline of the *de novo* assembly of bi-allelic loci used for *I.*
281 *nautilei* in Tran Lu Y et al (2022) following the procedure recommended by Mastretta-Yanes
282 et al. (2015) and Paris et al. (2017). After running several sets of parameter combinations, we
283 decided to use the assembly parameters that ranged between 4 and 6 for m, 4 and 11 for M
284 and 5 and 11 for n, depending on the species under scrutiny (see SI Calibration & SI Table 3).
285 In addition, we applied the same methodology, analyses, modules and filtering parameters
286 that we used for *I. nautilei* in Tran Lu Y et al. (2022) to better compare genetic patterns
287 between species (see SI Calibration). The *de novo* assemblies and subsequent filtering steps
288 resulted in a variable number of SNPs (2 904 to 47 547) obtained for 159 to 414 individuals
289 retained for each of the 7 species (see SI Table 2 & 3).

290

291 ***Population structure and admixture.***

292 Population structure analyses revealed similar patterns for the spatial distribution of genetic
293 diversity for the seven species. The PCA showed a common genetic structure, separating the
294 Manus individuals from those of the Eastern zones (i.e. North Fiji, Futuna and Lau, hereafter
295 NF/F/L) on the first component (PC1), with 1.94% to 26.03% of the total variance explained
296 (Figure 2). However, the site La Scala on the Woodlark Ridge (newly discovered, Boulart et al.,
297 2021) showed contrasting results. First, *I. nautilei*, *A. kojimai*, and *E. ohtai* are clearly
298 subdivided into two genetic groups with individuals of Manus-Woodlark (M/W) on one hand,
299 and individuals from NF/F/L on the other hand (Figure 2 A, B, D). However, the genetic
300 relationships of individuals from Woodlark differ slightly for the other species. *S. tollmanni*
301 was also subdivided into two genetic groups but individuals from Woodlark clustered with
302 either the Manus or with the NF/F/L genetic groups, with one admixed individual positioned
303 in between (Figure 2 E). For *L. schrolli & L fijiensis,* all individuals from Woodlark are positioned
304 as intermediates between Manus (*L. schrolli)* and NF/F/L (*L fijiensis)*. These intermediate
305 individuals are genetically closer to the North Fiji individuals, which slightly differed from the
306 Futuna/Lau (F/L) individuals on PC1 (Figure 2 G). A comparable situation also holds for the
307 species *B. segonzaci* for which the Woodlark individuals are well separated from either
308 individuals of Manus or those of the NF/F/L group but are a little bit closer to the latter (Figure
309 2 F). For *B. manusensis,* which is absent from La Scala, a similar situation is observed (Figure 2
310 C).

311 The second component (PC2) accounting for 0.62-0.76% of the total genetic variance, also
312 showed slight differences at the regional scale for some species (Figure 2 B, F, G). Individuals
313 from North Fiji exhibit a slight genetic differentiation from the group F/L on PC2 for both *A.*
314 *kojimai* and *L. fijiensis*, and the same pattern is observed between Woodlark and Manus
315 individuals for *B. segonzaci* and *L. schrolli.* According to the first two principal components of
316 the PCA, the only species exhibiting a more basin-specific signature was the species complex
317 *L. schrolli/L. fijiensis* (Figure 2 G and SI Figure 1).

318 This shared distribution of the genetic variation was also captured by admixture analyses for
319 all species. The optimal number of clusters identified was always k = 2 (SI Figure 2). These two
320 genetic units are composed, as previously found, of M/W individuals on one side, and NF/F/L
321 on the other side. Except for some individuals from Woodlark and North Fiji BABs for which
322 genome admixture ranged between 10 to 50% depending on the species under scrutiny, the
323 proportion of shared ancestry between these two groups is very low for most individuals
324 (Figure 2). Woodlark individuals for *L. schrolli/L. fijiensis, S. tollmanni* and *B. segonzaci* display
325 shared ancestry from both genetic clusters. In *S. tollmanni*, the Woodlark population is
326 composed of a mixture of parental types (both genetic backgrounds) and a putative F1 hybrid.
327 In contrast, all Woodlark individuals displayed almost equal (~50%) shared ancestry from both
328 *L. schrolli* (Manus group) and *L. fijiensis* (Eastern group) when k = 2. Admixture analyses also
329 discriminate additional clusters for Woodlark and then North Fiji in the *L. schrolli/L.fijiensis*
330 species complex with increasing values of k (K = 3 to 5, SI Figure 3 & 4).

331 The F_3 statistics showed significant negative values, indicating admixture in Woodlark, for two
332 species only. The first species is *S. tollmanni*, with individuals from the Western (Woodlark2)
333 population (Manus type) with source populations coming from both Manus (M) and the
334 Eastern group (NF/F/L) and Woodlark1 (Lau type). The Woodlark *Lepetodrilus* individuals
335 displayed a similar situation with source populations coming also from Manus (M) and the
336 Eastern group (NF/F/L) (SI Figure 5).

337 Examining the overall genetic differentiation (F_{st}) and the net divergences (D_a) between the
338 Western and Eastern groups provided three main patterns (Table 1). The first group of species
339 (i.e. the limpets *Lepetodrilus* and *Shinkailepas*) is characterized by high values of
340 differentiation (0.271-0.360) and divergence (0.013-0.019). The species of the second group
341 (*I. nautilei, E. ohtai* and *B. manusensis*) also have high values of genetic differentiation (0.203-

342 0.387) but low to moderate divergences (0.002-0.007). Finally, the last group comprising *B.*
343 *segonzaci* and *A. kojimai* has low values of genetic differentiation (0.018-0.038) and moderate
344 divergences (0.007).

345 Pairwise Fst also captured differentiation between localities, when the five regions were
346 considered as separate populations, with F_{st} ranging from 0 to 0.364, depending on the species
347 analyzed and the pair of populations compared (SI Table 4). Most cases of significant genetic
348 differentiation between BABs were observed in pairwise comparisons between the Western
349 and Eastern BABs (Manus or Woodlark against Lau, North Fiji and Futuna). Some
350 differentiation was also observed at the basin scale within a group with some specific
351 separation of the populations from North Fiji and Futuna/Lau for the species *A. kojimai* and *L.*
352 *fijiensis*. No population differentiation between Lau and Futuna has been however observed
353 except for *L. fijiensis*, where differentiation is extremely low but significant.

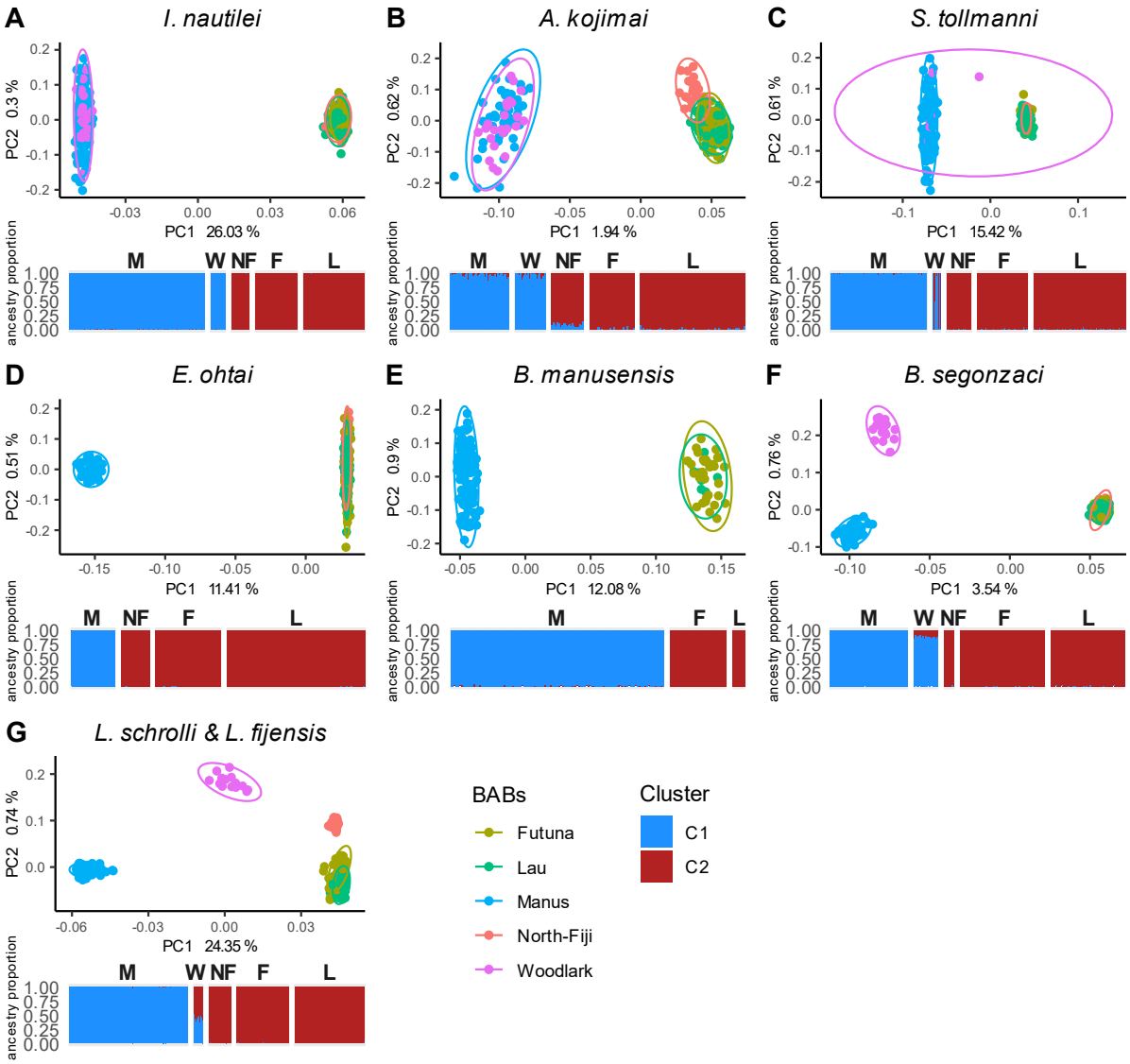

Figure 2: All PCA (PC1 & PC2) and Admixture plots for the best number of genetic clusters (K = 2) for each species (A, B, C, D, E, F , G). Colors in PCA plots represent regions (Manus, Woodlark, North Fiji and Lau Back-Arc-Basins, and the Futuna Volcanic Arc). Open circles represent the multivariate normal distribution of each group of points (basins) at 95% in PCA plots. Colors in Admixture plots represent each inferred genetic cluster. M: Manus, W: Woodlark, NF: North Fiji, F: Futuna, L: Lau.

366 *Table 1: Fixation index (Fst) and net nucleotide divergence (Da) measured between the two (Eastern and Western)*
367 *metapopulations for each species.*

Species	***F_{st}*** (M/W vs NF/F/L)	***Da*** (M/W vs NF/F/L)
Lepetodrilus schrolli & L. fijensis	0.360	0.019
Shinkailepas tollmanni	0.271	0.013
Ifremeria nautilei	0.387	0.008
Eochionelasmus ohtai	0.203	0.007
Branchinotogluma segonzaci	0.038	0.007
Alviniconcha kojimai	0.018	0.007
Bathymodiolus manusensis	0.206	0.002

368

369 Treemix analyses revealed a consistent two-group pattern of population differentiation across
370 species, with varying optimal numbers of migration events (ranging from 0 to 2) between the
371 two regions (SI Figure 6 and 7). These findings highlight the occurrence of a primary migration
372 event between the Eastern and Western groups for all species, excluding *E. ohtai* and *B.*
373 *manusensis*. Furthermore, a secondary migration event was exclusively observed for *I.*
374 *nautilei*, *A. kojimai*, and *S. tollmanni*, occurring between two different basins of the same
375 genetic group (i.e., metapopulation). Notably, these interacting basins were not consistently
376 the same across different species. *B. segonzaci* exhibited a distinctive pattern, featuring two
377 migration events between the Eastern and Western groups: the first one from Futuna to
378 Woodlark and the second from Lau to Manus.

379 ***Genetic diversity of species***

380 Regardless of the statistics used (Ho, He and π: SI figure 8 & 9), *S. tollmani* displayed a gene
381 diversity twice higher than that of the other species. The level of genetic diversity of species
382 slightly differed between the Eastern and Western groups, but not always in the same
383 direction. *I. nautilei*, *B. manusensis* and *L. schrolli/L.fijiensis* exhibit a slightly higher gene
384 diversity in M/W compared with NF/F/L whereas it was the opposite for the other species (*A.*
385 *kojimai*, *S. tollmani*, *E. ohtai* and *B. segonzaci*). These statistics displayed exactly the same
386 pattern of distribution when calculated per basin (see SI Figure 9).

387 ***Evolutionary history of populations and connectivity at the multispecies scale***

388 **Relative migration rates**

389 The Divmigrate analysis between the Eastern and Western groups revealed a robust and
390 common pattern of bidirectional but asymmetrical gene flow in all species. The main direction
391 of gene flow predicted by the analysis is westward from NF/F/L (1) to M/W (2), while gene
392 flow in the opposite direction was about half to a two-third (SI Figure 10). The species complex
393 *L. schrolli/L. fijiensis*, however, displayed a more complex bidirectional pattern with a much
394 stronger gene flow between Futuna and Lau than between Futuna/Lau and North Fiji and
395 virtually no gene flow between Woodlark, Manus and the others BABs.

396 **Demo-genetic inferences**

397 **Modes of divergence**

398 The folded JAFS (Figure 3) show the distribution of allelic variants between the Eastern and
399 western metapopulations for each species. Of the 28 models tested for each species, the SC
400 (Secondary Contact) model was almost always the best-fitting model selected by the
401 Weighted AIC. The exceptions are *I. nautilei* (Tran Lu Y et al., 2022) and *B. manusensis*, for
402 which the SC model is slightly, but not significantly, better than the IM (Isolation with
403 Migration) model. The Strict Isolation (SI) model was the worst model for all species. This
404 indicated that all species are still able to maintain low levels of gene flow at the regional scale
405 despite the large geographical distances and the abyssal plain separating the different regions.
406 Increasing the complexity of the SC or IM population model by the addition of genomic
407 heterogeneity (2N and/or 2m) or demographic change (G) parameters improved the model fit
408 (see Figure 4 and SI Figure 11). Capturing linked selection (2N) improved the model fit more
409 than the G or 2m parameters for most species except *E. ohtai*. Alternatively, adding
410 heterogeneous gene flow (2m) to the SC model improved the model fit for *E. ohtai* (SC2mG),
411 although the two metapopulations appeared to be well separated. This situation of semi-
412 permeable barrier also holds for *S. tollmanni* and *L. schrolli/L. fijensis,* for which genetic
413 admixture is locally suspected. For these two latter species but also for *A. kojimai*, *B.*
414 *segonzaci*, and *I. nautilei,* the SC2N2mG was the best model after evaluating all possible
415 parameter combinations. For *B. manusensis*, it was however not possible to discriminate

between the models IM2N, SC2N, and SC2N2m, and both SC2mG and SC2NG performed similarly as well as the SC2N2mG model for *B. segonzaci* (Figure 4 and SI Figure 11 & 12).

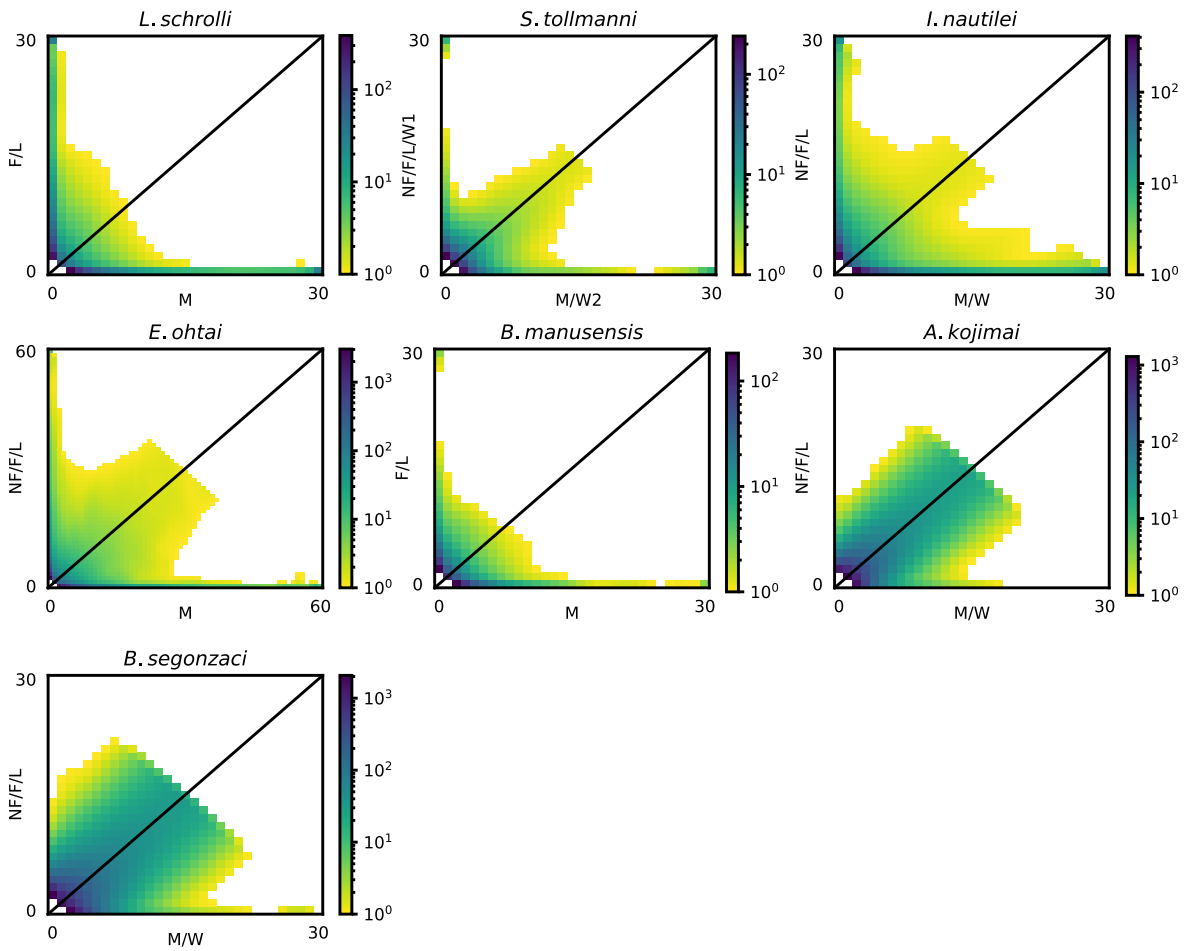

Figure 3: Folded Joint Allele Frequency Spectrum (JAFS) plots for all species. Each four plots represent, Observed Joint allele frequency spectrum (JAFS) between lineages East and West. NF: North Fiji, F: Futuna, L: Lau, M: Manus, W: Woodlark

Timing of divergence and gene flow

Depending on the best model, we estimated divergent times Ts (time since the population split), Tsc (time since the secondary contact after the primary divergence), and Ttotal (which could be Ts or Ts+Tsc), using a fixed mutation rate of 10^{-8} (Table 2). Ts ranged by a factor of ten thousand generations to about one hundred thousand generations according to the species analyzed (40 000 for *A. kojimai* to 116 000 for *L. schrolli/L. fijensis*). Similarly, the time elapsed since secondary contact (Tsc) changes also by a factor of 10 from 6,386 generations for *S. tollmanni* to 69,371 generations for *I. nautilei* and *L. schrolli/L. fijensis*. However, the total time since the ancestral population split (Ts or Ts+Tsc) varied less, with the lowest values being 40,892 and 42,117 generations for *A. kojimai* and *B. segonzaci* respectively, and the highest values being 94,071, 116,711 and 101,718 generations for *E. ohtai*, *L. schrolli/L. fijiensis* and *B. manusensis*, respectively. For *B. manusensis*, the time of divergence however varied up to two-fold (43,644 to 101,718

432 generations) depending on the best models used. *I. nautilei* and *S. tollmanni* produced intermediate values
433 of spitting times.

434 All species display heterogeneous gene flow (2m). Migration rate parameters estimated from *∂a∂i* show
435 that present-day gene flow is stronger from NF/F/L to M/W (East to West) than the opposite, with the
436 exception of *L. schrolli/L. fijiensis* for both the two classes of gene flow ("neutral" migration m and
437 "reduced" (due to barrier loci) migration me, in relative genomic proportions P and 1-P; Table 3). For *B.*
438 *manusensis*, migration rates were similar in both directions. *I. nautilei* and *E. ohtai* had about half of their
439 genome characterized by reduced gene flow (P ~=1-P). Only *A. kojimai* displayed high neutral gene flow
440 (with m>me and P>>1-P) whereas *S. tollmanni, B. segonzaci, B. manusensis and L. schrolli/L. fijiensis)*
441 exhibited a larger proportion of barrier loci (1-P >>P) which strongly reduced gene flow (me <<m) between
442 the genome of the two genetic groups (Table 3).

443 *Table 2: Estimation of divergence times (Times are estimated with a fixed mutation rate per generation and site, 10^{-8}) and*
444 *estimation of mutation rate per site and generation for all species. Ts: time since the ancestral population subdivided into two*
445 *populations; Tsc: time since secondary contact. Ttotal: Ts and Ts + Tsc. For I. nautilei using the AM2N2mG model, Ts*
446 *corresponds to the time of the strict split after ancient migration ended (Tsc).*

Species	Best model	Ts	**Tsc**	**Ttotal**
I. nautilei	IM2N2mG		66 951	66 951
I. nautilei	SC2N2mG	16 279	54 017	70 295
I. nautilei	AM2N2MG	41	69 372	69 413
A. kojimai	SC2N2mG	29 157	11 735	40 892
S. tollmanni	SC2N2m	63 335	5 419	68 754
S. tollmanni	SC2N2mG	42 683	22 326	65 009
E. ohtai	SC2mG	37 278	56 793	94 071
B. segonzaci	SC2N2mG	18 194	15 375	33 569
B. manusensis	IM2N	101 718		101 718
B. manusensis	SC2N2m	40 752	2 892	43 644
B. manusensis	SC2N	56 394	37 940	94 335
L. schrolli/L. fijensis)	SC2N2mG	48 381	68 331	116 712

447

448

449

450

451 *Table 3: Gene flow parameters estimated from ∂a∂i (m and me are the "neutral" and "reduced" migration rate parameters.*
452 *P the proportion of the genome characterized by migration rate m, and 1-P the proportion of the genome affected by reduced*
453 *migration me). 1 : East population (NF/F/L); 2 : West population (M/W).*

Species	Best model	m1<-2	m2<-1	P	me1<-2	me2<-1	1-P
I.nautilei	IM2N2mG	0,444	0,825	0,483	0,038	0,283	0,517
I.nautilei	SC2N2mG	0,422	0,810	0,439	0,038	0,270	0,561
I.nautilei	AM2N2MG	0,461	0,825	0,471	0,039	0,300	0,529
A. kojimai	SC2N2mG	4,741	4,389	0,851	0,384	0,841	0,149
S. tollmanni	SC2N2m	0,321	3,314	0,014	4,334	13,866	0,986
S. tollmanni	SC2N2mG	0,268	1,048	0,205	1,048	2,800	0,795
E. ohtai	SC2mG	0,364	1,386	0,508	0,013	0,124	0,492
B. segonzaci	SC2N2mG	0,579	6,489	0,000	2,195	5,412	1,000
B. manusensis	IM2N	0,436	0,566				
B. manusensis	SC2N2m	3,988	4,891	0,323	0,227	0,646	0,677
B. manusensis	SC2N	0,520	0,537				
L. schrolli/L. fijensis)	SC2N2mG	0,878	0,308	0,180	0,009	0,007	0,820

454

Figure 4 : Weighted AIC value on the best runs for all models and parameters per species. Highest value represents the best model fit (the lowest AIC value). Ifremeria nautilei data are derived from Tran Lu Y et al. (2022).

Discussion

Population genomics allowed us to gain a deeper understanding of factors that have shaped genetic variation within and between populations in a context of a discontinuous ridge system in a well-delimited biogeographic region. Our study was aiming to "put the geography (and more) into comparative population genomics" (from Edwards et al., 2022) by applying such an approach to seven very different taxa strictly associated with the hydrothermal habitat. Using the same sampling scheme across all species, we show that these species share a common biogeographic break and a similar demographic history despite their different life-history traits. This pattern of differentiation was however slightly more complex for the limpet

467 *L. schrolli/L. fijiensis, S. tollmanni and* the scaleworm *B. segonzaci*, for which a further genetic
468 subdivision between the Manus Basin and the Woodlark Ridge was also observed.

469 The multispecies transition zone between the Eastern and Western metapopulations is
470 located on the Woodlark Ridge or between it and the western part of the North Fiji BAB,
471 isolating the Manus Basin to the West and the North Fiji and Lau Basins, as well as the Futuna
472 volcanic arc to the East. Based on demogenetic inferences, we found that after a primary
473 allopatric divergence, these metapopulations were secondarily connected, resulting in weak,
474 asymmetric, and predominantly westward ongoing gene flow. Levels of divergence and
475 differentiation, however, varied between taxa, probably because of different generation times
476 and life-history traits. Heterogeneous gene flow was also found in all species in various
477 proportions, suggesting that primary divergence could have led to the generation of genomic
478 incompatibilities, as commonly found in hybrid zones (Bierne et al., 2011; Matute et al., 2010).

479

480 ***A suture zone around the Woodlark back-arc Basin.***

481 All seven species share a clear genetic break into two main metapopulations across their
482 geographical range, with the Manus/Woodlark (M/W) BABs on one hand and the North Fiji,
483 and Lau BABs and Futuna Volcanic Arc (NF/F/L) on the other hand. Despite this common
484 phylogeographic pattern, the strength of differentiation between these Eastern and Western
485 genetic pools estimated by F_{st} varied from very high (0.387) to very low (0.020), depending on
486 the species. A transition zone, a region where previously isolated lineages come into contact
487 and exchange genetic material, appears to be located somewhere between North Fiji and
488 Woodlark BAB or even at Woodlark itself, where both lineages are found in sympatry for some
489 species. This is clearly observed for the two limpet species complexes, *S. tollmanni* and *L.*
490 *schrolli/L. fijiensis*, for which the Western and Eastern lineages co-occur in Woodlark and
491 hybrid individuals, are detected. This signature is typical of the existence of a tension zone,
492 where selection can operate against hybrid genotypes, probably due to the existence of
493 underdominant genetic incompatibilities (Bierne et al., 2011) or other reproductive barriers.
494 Variable levels of admixture detected between Western and Eastern lineages in all species
495 present at Woodlark, and, to a lesser extent at North Fiji (Tran Lu Y et al. 2023), reinforced this
496 view. The species variability in terms of population structuring can stem from diverse origins:
497 differences in life history traits (generation time, dispersal capability, fecundity, ...) or in the
498 genomic architecture of species (intensity of linked selection and number of barrier loci

499 (genetic incompatibilities) that whole genome information could help better visualize. These
500 latter factors are noticeably linked with the depth of evolutionary history of divergence and
501 the reproductive mode. Our study suggests two possible hypotheses. First, geophysical
502 rearrangements at a given time may have limited (and are still currently limiting) effective
503 dispersal for a number of species with different life history traits. Leading this common pattern
504 of isolation, regardless of the timing of their origin in the SouthwesternPacific (isolation with
505 migration, IM, one of the models supported by *∂a∂i* for *Ifremeria nautilei* and *Bathymodiolus*
506 *manusensis*). Alternatively, these species may have experienced one or more vicariance
507 events, resulting in a period of primary divergence in allopatry followed by secondary contacts
508 (SC) with a gene flow restart. The latter scenario is the most likely, supported by the *∂a∂i*
509 analyses for most species (Figures 3 & 4).

510 While evolutionary processes unfold independently in each species, our demogenetic
511 reconstruction indeed indicates a scenario of secondary contact (SC) for five species. For two
512 species, the model cannot decisively distinguish between secondary contact and isolation-
513 with-migration (IM), possibly due to a prolonged period of secondary contact. These results
514 nevertheless strongly suggest an allopatric initial divergence for all species. Modeling also
515 underscored the detection of a genomic heterogeneity of differentiation in all species, with
516 both heterogeneous gene flow across the genome (2m) and linked selection (2N). This finding
517 suggests that the initial divergence was extensive enough to generate genomic
518 incompatibilities between populations in a genome characterized by substantial background
519 selection and low recombination. This pattern can be a feature of hydrothermal-vent species,
520 which may undergo strong purifying selection in this challenging environment (Chevaldonné
521 et al. 2002, Fontanillas et al. 2017, Thomas-Bulle et al. 2022).

522 The position of the contact zone between Western and Eastern lineages, today located at
523 Woodlark or closeby, may have moved since the secondary contact took place, probably along
524 the subduction arcs of Vanuatu or Solomon. Nevertheless, the Manus Basin appears more
525 diversified in terms of species (Poitrimol et al., 2022) and could have served as a source of
526 biodiversity for part of the Western Pacific hydrothermal fauna, suggesting a possible "out of
527 Manus" hypothesis. In line with this idea, recent work on taxa network analysis redescribes
528 the Western Pacific region for hydrothermal fauna not as a single biogeographic province, as
529 suggested by Moalic et al. (2012), but as two distinct provinces, the North West Pacific and

530 the South West Pacific, with the Manus Basin as a possible hub connecting both (Tunnicliffe
531 et al., 2024).

532 ***Gene flow between BABs***

533 The connectivity and dispersal of hydrothermal vent species may be influenced by their life
534 history traits, particularly the larval phase. Species with planktotrophic larvae, which can have
535 an extended planktonic phase, should exhibit higher dispersal abilities and greater
536 connectivity between populations. In contrast, species with lecithotrophic larvae, which rely
537 on yolk reserves and usually have a shorter planktonic phase in coastal waters, are expected
538 to show more limited dispersal and reduced connectivity (but see: Young 1994 for the deep-
539 sea fauna). Our findings, with a consistent asymmetrical gene flow (lower eastward gene
540 flow), unequivocally reject complete isolation between East and West
541 metapopulation/lineages for all species, despite their contrasting dispersal life-traits. It
542 partially also aligns with prior studies indicating very low gene flow between Manus and Lau
543 BABs (Breusing et al., 2021; Plouviez et al., 2019; Thaler et al., 2011, 2014). However some
544 other studies have reported a lack of genetic differentiation for *S. tollmanni* with some mito-
545 nuclear incongruities (Yahagi etl., 2019, Poitrimol et al., 2022). Additionally, our demogenetic
546 modeling indicates semi-permeability (2m) of gene flow for all species, probably from the
547 accumulation of genomic incompatibilities and other barrier loci during primary divergence
548 preceding secondary contact (Barton & Bengtsson, 1986).

549 The orientation of gene flow also partially aligns with previous simulations of larval dispersal
550 at intermediate depth (Mitarai et al., 2016). However, the bi-directional nature of the gene
551 flow suggests potential dispersal near the surface, where the main counter-current flows
552 eastward, in addition to the deep-water westward dispersal. The current genetic data and the
553 lack of information on the biology of the species are insufficient to assess the role of life-
554 history traits, particularly the larval developmental mode of the species, in relation to the
555 degrees of differentiation, divergence, or even the orientation of dispersal at this stage.
556 Further analyses are required with a better understanding of the biology of these species.
557 Depending on the life-history traits and potential presence of intermediate populations in the
558 Vanuatu and Solomon archipelagos, the frequency and duration of secondary contacts may
559 have varied between the Eastern and Western lineages. Nevertheless, present-day
560 connectivity remains highly limited due to the existence of both genetic and physical barriers
561 to dispersal. In this scenario, species with high dispersal abilities and/or long generation times

562 may have experienced less divergence (e.g., *A. kojimai, B. segonzaci)* compared to those with
563 low dispersal abilities and short generation times (e.g., *L. schrolli/L. fijiensis*). This situation is
564 well illustrated in vent copepods in the Lau Basin, which possess both of the latter attributes
565 (Diaz-Recio Lorenzo et al., 2024).

566 **Species specific variation**

567 While the West/East divergence is clear for all species, few species display some basin
568 peculiarities.

569 *B. segonzaci* shows slight differentiation between Woodlark and Manus Basin populations,
570 not solely due to allelic introgression from other Eastern regions. The North Fiji Basin
571 population of *A. kojimai* differs slightly from the Lau/Futuna regions, despite the overall lack
572 of genetic differentiation (Fst= 0.018) at the regional scale. *B. manusensis* has been newly
573 identified in the Eastern regions (north of Lau Basin and Futuna volcanic arc). This unusual
574 presence in the East is notable, as it locally co-occurred with *B. septemdierum*: the only mussel
575 species typically found in that area. These Eastern scattered populations may represent a
576 leading edge of range expansion but lack the expected reduced diversity (Dupoué et al., 2020).
577 The slight basin differentiation for *B. segonzaci* and *A. kojimai* raises questions about limiting
578 factors on connectivity, potentially influenced by larval dispersal depth, demographic turn-
579 over, or putative depth selection in North Fiji Basin and Woodlark populations.

580 While most of our species exhibit a relatively low level of genetic divergence, the limpets *L.*
581 *schrolli/L. fijiensis* and *S. tollmanni* show a high degree of divergence and differentiation, as
582 well as a highly reduced gene flow between the Western and Eastern groups. *S. tollmanni*
583 displays a clear admixture signal in Woodlark, where both lineages are in sympatry and one
584 first generation hybrid was identified. Previous studies have shown a lack of genetic
585 differentiation at the regional scale with the mitochondrial *Cox1* (Poitrimol et al., 2022; Yahagi
586 et al., 2020). Based on genomic data, the two lineages West/East are strongly isolated and
587 display very reduced and heterogeneous gene flow, where alleles can be exchanged at very
588 few loci. This incongruity is consistent with our results. Indicating a strong reduction in gene
589 flow, but where few loci can still be exchanged and captured, including mitochondrial
590 genomes.

591 The species *L. schrolli* and *L. fijiensis* display a nearly identical divergence but with a clearly
592 admixed population between the Manus and NF/F/L lineages at Woodlark. This result is in line
593 with mtDNA *Cox1* results for Woodlark individuals, where half of them reflect Manus *Cox1*
594 haplotype lineage and the other half, the NF/F/L haplotype one (Poitrimol et al., 2022). This
595 is also consistent with previous results using 42 nuclear markers, which indicate very low and
596 asymmetric gene flow between Manus and Lau BABs (Plouviez et al 2019). It indicates
597 segregation for mtDNA markers in a sympatric population, consistent with the possible partial
598 accumulation of genomic incompatibilities in which the mitochondrial genome is this time
599 included. Our findings therefore reinforce the recent taxonomic revision of *L. schrolli* (M) and
600 *L. aff schrolli*, now *L. fijiensis* (NF/F/L), as separate species (Chen & Sigwart 2023). This also
601 suggests that the taxonomy of *S. tollmanni* may need some revision.

602 As previously mentioned, dispersal-related life history traits potentially influence connectivity.
603 However, when we look at what we know about the life history traits of our seven species,
604 there is no consistency with the type of larval development. *B. segonzaci* and *A. kojimai*, both
605 colonizing the hottest parts of the West Pacific vent environment, display the lowest genetic
606 differentiation and divergence between Eastern and Western populations, despite having
607 different larval development modes. *B. segonzaci* is a free-living, mobile annelid with small
608 local population sizes. Its large oocytes (ca. 150 µm) suggest lecithotrophic larval development
609 that can remain for long times in cold oligotrophic waters. *A. kojimai*, on the other hand, has
610 larger patchily distributed populations and produces much smaller oocytes, implying
611 planktotrophic larval development in surface waters (Warèn & Bouchet, 1993, Sommer et al.
612 2017, Kim et al., 2022). In these two species, the low level of regional differentiation therefore
613 could be linked to the specific distribution of 'hot' vent emissions when compared to colder
614 diffuse venting, provided that they are both able to widely disperse.

615 *B. manusensis* and *E. ohtai* also display a low level of divergence, but exhibit an intermediate
616 level of differentiation between metapopulations. *E. ohtai* is a common sessile hydrothermal
617 vent cirriped forming dense populations in diffuse areas. Its oocyte diameter (ca. 500 µm)
618 again suggests lecithotrophic development (~500 µm; SH unpublished data, Yamaguchi &
619 Newman 1997, Tyler & Young 1999). In contrast, deep-sea bivalves such *as B. manusensis*
620 typically have small oocytes and larvae are expected to be planktotrophic, as larvae of
621 *Gigantidas childressi* (formerly known as "*Bathymodiolus*" *childressi*) have been detected in
622 surface water and known to live up to 18 months (Arellano and Young, 2009).

623 Although the focus was on the Southwest Pacific BABs, the Kermadec Basin, hundreds of
624 nautical miles south of the Lau Basin, has a very distinctive vent fauna. But, *B. segonzaci* and
625 *L. fijiensis* are among the very few species shared with the most northerly location sampled
626 here (SH unpublished data). It therefore appears that these species may have spread for a
627 longer time and/or have greater habitat flexibility than other species. The addition of some
628 individuals from Kermadec to the dataset showed no differentiation from the NF/F/L
629 population for *B. segonzaci*, but did show some differentiation from NF/F/L for *L. fijiensis* (see
630 details in SI Figures 13, 14, 15, data not shown).

631 ***Timing divergences and the hypothesis of vicariance***

632 The comparative study highlights common phylogeographic patterns across the Southwest
633 Pacific Ocean for seven vent species. This pattern has probably been generated by a shared
634 initial divergence event, due to either geological or climatic factors, generating two
635 metapopulations, with the separation lying somewhere between Woodlark and North Fiji
636 BABs, if we consider the populations have remained in place during the isolation process. This
637 barrier is semi permeable to gene flow, allowing occasionally metapopulations to exchange
638 genetic material through secondary contacts but not at the same rate and not over the same
639 regions of their genomes. This reconnection may also be modulated by species-specific life-
640 history traits, including type of larval development (planktotrophic vs. lecithotrophic), depth
641 of larval dispersion, longevity, age of first reproduction and mean generation time or habitat
642 fragmentation.

643 The estimation of net nucleotide divergence (*Da*), shows that species have undergone
644 different periods of divergence. In particular, *L. schrolli/L. fijiensis)* and *S. tollmanni* both
645 display particularly high net divergence values compared to the other species. This indirect
646 approach suggests that these two species did undergo a longer period of isolation in allopatry
647 or a much higher number of generations since a possible vicariant event. These results
648 naturally pose the question of cryptic species and speciation processes. This level falls into the
649 grey zone of speciation of Roux et al. (2017), where reproductive isolation between
650 populations varies widely. Our demogenetic inferences shed some light not only on the
651 intensity and genomic heterogeneity of gene flow (as previously discussed) but also on the
652 timing of divergence.

653 The divergence time since the ancestral lineage split, in generations, indeed varies by a factor
654 of three between species even if they all share the same population history. In this approach,
655 time estimation strongly depends on the per generation nucleotide mutation rate and the
656 mean generation time considered for each species. However, these biological parameters not
657 yet known for the species studied here. This is a common limitation for many non-model
658 organisms (and especially in the deep-sea), and has led us to make assumptions for both
659 parameters that we have set to the same value for all species, although we acknowledge this
660 is highly unlikely. Thus, a factor of three in the divergence time is not so great and can be
661 largely due to the distinct species life history traits. Some studies on growth rates show that
662 larger species have slower growth rates (Schöne & Giere, 2005), while small ones have higher
663 rates (Poitrimol et al., 2024), suggesting discrepancy in the generation time and first age at
664 maturity between species. In addition, bigger species often have smaller population sizes than
665 smaller ones and we cannot exclude the possibility that they would have otherwise undergone
666 relatively simultaneous demographic changes.

667 Resulting estimates of primary divergence may have begun between ~ 40,892 to 101,718
668 generations, while the secondary contact ranges from 6,386 to 69,372 generations, depending
669 on the species. Considering an average mutation rate of 10^{-8} and a quite short time of one
670 generation per year, this primary divergence and secondary contact would take place in the
671 Holocene between climatic oscillations. The initial split may be more specifically around the
672 Last Glacial Maxima for the region (11,500-20,300 years ago (Tongo Glaciation), 62,000 years
673 ago (Komia Glaciation) and 130,600-158,000 years ago (Mengane Glaciation) (Barrows et al.,
674 2011)).

675 At the other end of the range. If we consider a ten times lower mutation rates (10^{-9}) that has
676 been largely invoked in the molecular dating of the vent fauna as the result of strong purifying
677 selection (Chevaldonné et al. 2002, Johnson et al. 2006, Matabos and Jollivet 2019). The
678 magnitude of divergence would be in the order of 400,000 to 1,000,000 years and 63,860 -
679 693,720 for the secondary contact. This primary divergence timeframe falls partly at the start
680 of magmatic accretion in some actual active BAB ridges, such as Lau or Manus (Schellart et al.,
681 2006). The geological structures that currently separate the two genetic entities are the
682 Woodlark Basin, North-Fiji and the other geological structures between them (Vanuatu
683 Trough (formerly New Hebrides), Vanuatu and Solomon Islands volcanic arc). These
684 formations have a rather older geotectonic history with accretion times of several million

685 years (Woodlark: ~ 6 Ma, North Fiji: ~3Ma, Vanuatu Trough & volcanic arc: 12Ma, Solomon
686 volcanic arc: Eocene, ~ 40 Ma) (Schellart et al., 2006). While this primary divergence period
687 better fits these geodynamic features, the time frame for secondary contact still remains in
688 the Holocene period and may be the consequences of climatic oscillations and possible
689 changes in the overall Pacific water-mass circulation due to the ocean elevation.

690 Timeframe estimates remain very difficult to interpret due to many unknowns on the biology
691 of the species, but all species were affected, suggesting a major climatic or geological
692 reorganization of connectivity that probably initiated the primary divergence and the
693 secondary contact. However, we cannot reject the hypothesis that some secondary contacts
694 are much older than others since life-traits history varies between species.

695 ***Limits of the method and other hydrothermal species***

696 The present study primarily focused on the most common and emblematic species in
697 hydrothermal communities. Earlier studies on two of our target species and other
698 hydrothermal vent inhabitants have yielded findings consistent with our results (Lee et al.,
699 2019; Plouviez et al. 2019; Poitrimol et al., 2022; Thaler et al., 2014). Like all our species, they
700 exhibit a 'common' pattern of genetic differentiation across the Western and Eastern parts of
701 this region, implying a shared vicariant event. However, it is important to note that these
702 results may primarily reflect the evolutionary history of the most highly abundant vent
703 species. As mentioned earlier, these ecosystems are home to numerous other species. Many
704 of them probably have lower population densities, are less dependent on vent fluids and have
705 diversified much more rapidly towards endemism. Consequently, these less abundant and
706 often smaller species may demonstrate more contrasted phylogeographic patterns. For
707 example, based on *Cox1* data, some limpets, barnacles, and copepods have been shown to
708 have a wide distribution, while others (sometimes closely related) have a basin-specific
709 occurrence (Boulart et al., 2022; Poitrimol et al., 2022, Diaz-Recio Lorenzo et al. 2024).

710 Beyond the idea that we did not examine rare and occasional species, our comparative
711 phylogeographic study also has some limitations. First, our sampling design, although quite
712 extensive, focused on a fraction of the existing hydrothermal vents, lacking fine-grained
713 representation within and across BABs. This limitation is common in deep-sea research, where
714 potential habitats and populations are known or suspected but remain unsampled. In our
715 case, the study area comprised a few unsampled - documented vents (e.g. Nifonea in

716 Vanuatu), and other 'ghost' undiscovered vent sites possibly located on seamounts along
717 volcanic arcs. Additional data from these sites should not affect our main conclusions, but
718 they would provide useful information to refine our patterns of population connectivity and
719 the timing of contact zones. Second, we generated ddRAD datasets across a wide range of
720 species with significant divergence between geographic lineages. These varying contexts of
721 divergence may have influenced our results, as divergent lineages may share fewer ddRAD loci
722 due to allele dropout and preferential bias towards less divergent loci to avoid missing data,
723 although the number of remaining loci was still very high.

724 ***Implications for conservation and future directions***

725 As previously shown, cases that correspond to geographically separated cryptic species need
726 to be managed separately (e.g. *L. schrolli/L. fijiensis* or *S. tollmanni*). Other species depict much
727 lower divergence but with some variation in population differentiation. Although sporadic and
728 possibly rare, there is now clear evidence of present-day genetic connectivity between the
729 Western and Eastern metapopulations with an apparent high genetic homogeneity within
730 each of them. If larval exchange does not seem to be limited within each geographic group,
731 the inter-metapopulation migration rate is probably too low to allow any regional rescue
732 effect. Discussing effective migration and thus dispersal is however still quite challenging
733 (Lowe & Allendorf, 2010; Waples & Gaggiotti, 2006). Recent studies based on simulations of
734 particle dispersion at different depths (500 and 1000 meters) for *I. nautilei* and *Alviniconcha*
735 spp. suggested low but possible migration between BABs depending on the Pelagic Larval
736 Duration (PLD) and depth (Breusing et al., 2021; Mitarai et al., 2016). However, based on our
737 finding any rescue effect is likely to be basin-specific and highly sensitive to increasing local
738 extinctions magnified by deep-sea mining.

739 Most of our knowledge on the stability of vent ecosystems through time is derived from times
740 series established on the East Pacific Rise, a fast-spreading mid-oceanic ridge with a one-
741 dimensional stepping-stone axis of colonization (Dupreez & Fisher 2018, Audzijonyte &
742 Vrijenhoek 2011) and, some punctual physical barriers to dispersal (Plouviez et al. 2009, 2010,
743 2013). There, the fast extinction and recolonization rates of active sites are likely to select for
744 species, which can disperse far, and grow and reproduce fast. In back-arc basins, the ridge
745 spreading rate is rather low but varies between basins (Dick 2019). Extinction and
746 recolonization events are likely less common, which led to concerns about the ability of the
747 populations to recover if the metal sulfide deposits formed by the hydrothermal vent activity

748 are mined (Dupreez & Fisher 2018). Within each of the two metapopulations, high genetic
749 homogeneity of local populations can arise from either a substantial population size mitigating
750 genetic drift or the presence of a sufficient number of migrants exchanged within BABs.
751 Consequently, dispersal seems to be effective between nearby sites at the scale of either the
752 Western or Eastern regions, but much more limited between them. Because BAB zones are
753 spatially limited with a restricted number of active vent sites, mining the already known sites
754 should compromise any local 'rescue' effect. The fact that introgressed alleles between
755 metapopulations appear capable of reaching the Woodlark and North Fiji BABs only, suggests
756 that the inter-basin dispersal will not compensate for population bottlenecks within each
757 metapopulation. As shown by Bailleul et al. (2018), the apparent genetic homogeneity of
758 demes within a metapopulation is often maintained by a limited genetic drift, even in the face
759 of low inter-deme migration rates.

760 **Conclusion**

761 We have identified a strong phylogeographic break for several hydrothermal species of the
762 Southwest Pacific back-arc basins, consistent with a common suture zone between the
763 Woodlark and Lau basins. Although sharing a common pattern of population structuring,
764 variability in the degree of population differentiation is observed among these species,
765 potentially related to life history traits and species-specific demographic histories.

766 Our initial hypothesis that hydrothermal species of the Southwestern Pacific back-arc basins
767 may have evolved toward long-distance dispersal strategies to cross over non-hydrothermal
768 abyssal zones associated with a discontinuous system of oceanic ridges may only be valid for
769 a few species. In fact, the western Pacific vent communities are composed of species with
770 highly contrasted life-history traits and dispersal strategies, which are likely to promote the
771 good replenishment of populations locally in spite of vent instability, fragmentation and
772 geological discontinuities. Although some uncertainty remains about the timing of divergence
773 and secondary contacts, connectivity patterns between the two geographic groups are similar
774 among species, with asymmetric but bidirectional gene flow favoring the Western direction
775 (with the exception of *L. schrolli/L. fijiensis* for which a Manus origin of colonization is
776 suspected). This study clearly identified the existence of genetic barriers at some intermediate
777 locations that are likely to slow down gene flow for some species. It also confirmed that most
778 of the vent assemblages sustainability rather depends on the strength of the network of local

779 populations that makes up each regional metapopulation, rather than long distance dispersal.
780 Ensuring the resilience of these communities requires sustainable management of their
781 populations at the level of each biogeographic unit or back-arc basin, bearing in mind that the
782 majority of current genetic exchange between the Eastern and Western basins are more
783 specifically redirected towards the Manus Basin.

784 Acknowledgements

785 The research was funded by the ANR CERBERUS project (ANR-17-CE02-0003). We would like
786 to thank the captains and crews of the French research vessel *L'Atalante* and the ROV *Victor*
787 team for the CHUBACARC cruise (Hourdez and Jollivet, 2019,
788 https://doi.org/10.17600/18001111). Sampling would not have been possible without their
789 dedication. Shiptime and scientist travels were supported by the Flotte Océanographique
790 Française (FOF) and the Centre National de la Recherche Scientifique (CNRS). This work
791 benefited from access to the Genomer and ABIMS platforms part of the Biogenouest network,
792 at Station Biologique de Roscoff, an EMBRC-France and EMBRC-ERIC site. We also warmly
793 thank Cindy L. Van Dover for sharing with us some of her Manus 2009 samples in order to
794 perform preliminary ddRAD libraries over the different species to choose restriction enzymes
795 and check the number of usable loci.

796 Author contributions

797 Stephane Hourdez and Didier Jollivet designed the CHUBACARC and CERBERUS projects,
798 François Bonhomme supervised the genetic work. Adrien Tran Lu Y, Stéphanie Ruault, Claire
799 Daguin-Thiébaut, Anne-Sophie le Port, Marion Ballenghein, Sophie Arnaud-Haond, Jade
800 Castel, Camille Poitrimol, Eric Thiébaut, François Lallier, Thomas Broquet, François
801 Bonhomme, Didier Jollivet and Stéphane Hourdez performed laboratory work. Adrien Tran Lu
802 Y performed bioinformatic statistical analyses with the contribution of François Bonhomme,
803 Didier Jollivet, Pierre-Alexandre Gagnaire, Nicolas Bierne and Thomas Broquet. Adrien Tran
804 Lu Y, François Bonhomme, Thomas Broquet, Didier Jollivet and Stephane Hourdez wrote the
805 manuscript with feedback and inputs from all authors. All authors approved the manuscript

806 Conflict of interest

807 The authors have no conflicts of interest.

Data availability statement

Raw sequence reads (Individual fastq files) are available at the European Nucleotide Archive (bioproject PRJEB47533; *I. nautilei*) and the NCBI sequence read archive (PRJNA768636 for A. kojimai; PRJNA779874 for *L. schrolli*; PRJNA772682 for *S. tollmanni*; PRJNA1044574 for *B. manusensis*; PRJNA1030156 for *E. ohtai*; PRJNA1044042 for *B. segonzaci*). Metadata relative to the samples are also available with Biosamples accessions and linked to the sequence reads accessions. Scripts used in this study (R, ∂a∂i) are available on a public Github repository: (https://github.com/Atranluy/Scripts-Ifremeria). VCFs and associated metadata will be available on public repository upon peer-review and publication.

Benefit-sharing statement

In order to obtain the requested authorizations to work in national waters and in agreement with the Nagoya protocol, we contacted the authorities of the different countries (Papua-New Guinea, Fiji, and Tonga) and territories (Wallis and Futuna) for benefit sharing where sampling was performed. The data generated will be accessible on public databases (see above). The results obtained will also be communicated to these authorities which may have to make decisions regarding conservation of deep-sea hydrothermal vent communities in their EEZs. Observers for the different countries who took part in the on-board activities will be informed of our findings.

Bibliography

Alexander, D. H., & Lange, K. (2011). Enhancements to the ADMIXTURE algorithm for individual ancestry estimation. *BMC Bioinformatics*, *12*(1), 246. https://doi.org/10.1186/1471-2105-12-246

Arellano, S. M., & Young, C. M. (2009). Spawning, Development, and the Duration of Larval Life in a Deep-Sea Cold-Seep Mussel. *The Biological Bulletin*, *216*(2), 149-162. https://doi.org/10.1086/BBLv216n2p149

Audzijonyte, A., & Vrijenhoek, R. C. (2010). When Gaps Really Are Gaps : Statistical Phylogeography of Hydrothermal Vent Invertebrates. *Evolution*, *64*(8), 2369-2384. https://doi.org/10.1111/j.1558-5646.2010.00987.x

Avise, J. C. (2000). *Phylogeography : The History and Formation of Species*. Harvard University Press. https://doi.org/10.2307/j.ctv1nzfgj7

Avise, J. C. (2009). Phylogeography : Retrospect and prospect. *Journal of Biogeography*, *36*(1), 3-15. https://doi.org/10.1111/j.1365-2699.2008.02032.x

Avise, J. C., Arnold, J., Ball, R. M., Bermingham, E., Lamb, T., Neigel, J. E., Reeb, C. A., & Saunders, N. C. (1987). INTRASPECIFIC PHYLOGEOGRAPHY : The Mitochondrial DNA Bridge Between Population Genetics and Systematics. *Annual Review of Ecology and Systematics*, *18*(1), 489-522. https://doi.org/10.1146/annurev.es.18.110187.002421

Bachraty, C., Legendre, P., & Desbruyères, D. (2009). Biogeographic relationships among deep-sea hydrothermal vent faunas at global scale. *Deep Sea Research Part I: Oceanographic Research Papers*, *56*(8), 1371-1378. https://doi.org/10.1016/j.dsr.2009.01.009

Bailleul, D., Mackenzie, A., Sacchi, O., Poisson, F., Bierne, N., & Arnaud-Haond, S. (2018). Large-scale genetic panmixia in the blue shark (*Prionace glauca*) : A single worldwide population, or a genetic lag-time effect of the “grey zone” of differentiation? *Evolutionary Applications*, *11*(5), 614-630. https://doi.org/10.1111/eva.12591

Barrows, T. T., Hope, G. S., Prentice, M. L., Fifield, L. K., & Tims, S. G. (2011). Late Pleistocene glaciation of the Mt Giluwe volcano, Papua New Guinea. *Quaternary Science Reviews*, *30*(19-20), 2676-2689. https://doi.org/10.1016/j.quascirev.2011.05.022

Barton, N., & Bengtsson, B. O. (1986). The barrier to genetic exchange between hybridising populations. *Heredity*, *57*(3), Article 3. https://doi.org/10.1038/hdy.1986.135

Beaulieu, S. E., Baker, E. T., German, C. R., & Maffei, A. (2013). An authoritative global database for active submarine hydrothermal vent fields. *Geochemistry, Geophysics, Geosystems*, *14*(11), 4892-4905. https://doi.org/10.1002/2013GC004998

Bierne, N., Welch, J., Loire, E., Bonhomme, F., & David, P. (2011). The coupling hypothesis : Why genome scans may fail to map local adaptation genes. *Molecular Ecology*, *20*(10), 2044-2072. https://doi.org/10.1111/j.1365-294X.2011.05080.x

Breusing, C., Johnson, S. B., Mitarai, S., Beinart, R. A., & Tunnicliffe, V. (2021). Differential patterns of connectivity in Western Pacific hydrothermal vent metapopulations : A

comparison of biophysical and genetic models. *Evolutionary Applications*. https://doi.org/10.1111/eva.13326

Carver, R., Childs, J., Steinberg, P., Mabon, L., Matsuda, H., Squire, R., McLellan, B., & Esteban, M. (2020). A critical social perspective on deep sea mining : Lessons from the emergent industry in Japan. *Ocean & Coastal Management*, *193*, 105242. https://doi.org/10.1016/j.ocecoaman.2020.105242

Castel, J., Hourdez, S., Pradillon, F., Daguin-Thiébaut, C., Ballenghien, M., Ruault, S., Corre, E., Tran Lu Y, A., Mary, J., Gagnaire, P.-A., Bonhomme, F., Breusing, C., Broquet, T., & Jollivet, D. (2022). Inter-Specific Genetic Exchange Despite Strong Divergence in Deep-Sea Hydrothermal Vent Gastropods of the Genus Alviniconcha. *Genes*, *13*(6), Article 6. https://doi.org/10.3390/genes13060985

Chen, C., & Sigwart, J. D. (2023). The lost vent gastropod species of Lothar A. Beck. *Zootaxa*, *5270*(3), Article 3. https://doi.org/10.11646/zootaxa.5270.3.2

Chevaldonné, P., Jollivet, D., Desbruyères, D., Lutz, R., & Vrijenhoek, R. (2002). Sister-species of eastern Pacific hydrothermal vent worms (Ampharetidae, Alvinellidae, Vestimentifera) provide new mitochondrial COI clock calibration. *CBM - Cahiers de Biologie Marine*, *43*(3-4), 367-370. https://archimer.ifremer.fr/doc/00000/895/

Daguin-Thiébaut, C., Ruault, S., Roby, C., Broquet, T., Viard, F., & Brelsford, A. (2021, septembre 21). *Construction of individual ddRAD libraries*. Protocols.Io. https://www.protocols.io/view/construction-of-individual-ddrad-libraries-bv4tn8wn

De Jode, A., Le Moan, A., Johannesson, K., Faria, R., Stankowski, S., Westram, A. M., Butlin, R. K., Rafajlović, M., & Fraïsse, C. (2023). Ten years of demographic modeling of divergence and speciation in the sea. *Evolutionary Applications*, *16*(2), 542-559. https://doi.org/10.1111/eva.13428

Desbruyères, D., Hashimoto, J., & Fabri, M.-C. (2006). Composition and Biogeography of Hydrothermal Vent Communities in Western Pacific Back-Arc Basins. In *Back-Arc Spreading Systems : Geological, Biological, Chemical, and Physical Interactions* (p. 215-234). American Geophysical Union (AGU). https://doi.org/10.1029/166GM11

Diaz-Recio Lorenzo, C., Tran Lu Y, A., Brunner, O., Arbizu, P. M., Jollivet, D., Laurent, S., & Gollner, S. (2024). Highly structured populations of copepods at risk to deep-sea mining : Integration of genomic data with demogenetic and biophysical modelling. *Molecular Ecology*, *33*(9), e17340. https://doi.org/10.1111/mec.17340

Dick, G. J. (2019). The microbiomes of deep-sea hydrothermal vents : Distributed globally, shaped locally. Nature Reviews Microbiology, 17(5), 271-283. https://doi.org/10.1038/s41579-019-0160-2

Du Preez, C., & Fisher, C. R. (2018). Long-Term Stability of Back-Arc Basin Hydrothermal Vents. *Frontiers in Marine Science*, *5*. https://doi.org/10.3389/fmars.2018.00054

Dupoué, A., Trochet, A., Richard, M., Sorlin, M., Guillon, M., Teulieres-Quillet, J., Vallé, C., Rault, C., Berroneau, M., Berroneau, M., Lourdais, O., Blaimont, P., Bertrand, R., Pottier, G., Calvez, O., Guillaume, O., Le Chevalier, H., Souchet, J., Le Galliard, J.-F., … Aubret, F. (2021). Genetic and demographic trends from rear to leading edge are explained by climate and forest cover in a cold-adapted ectotherm. *Diversity and Distributions*, *27*(2), 267-281. https://doi.org/10.1111/ddi.13202

Edwards, S. V., Robin, V. V., Ferrand, N., & Moritz, C. (2022). The Evolution of Comparative Phylogeography : Putting the Geography (and More) into Comparative Population Genomics. *Genome Biology and Evolution*, *14*(1), evab176. https://doi.org/10.1093/gbe/evab176

Ewing, G. B., & Jensen, J. D. (2016). The consequences of not accounting for background selection in demographic inference. *Molecular Ecology*, *25*(1), 135-141. https://doi.org/10.1111/mec.13390

Excoffier, L., & Lischer, H. E. L. (2010). Arlequin suite ver 3.5 : A new series of programs to perform population genetics analyses under Linux and Windows. *Molecular Ecology Resources*, *10*(3), 564-567. https://doi.org/10.1111/j.1755-0998.2010.02847.x

Faure, B., Jollivet, D., Tanguy, A., Bonhomme, F., & Bierne, N. (2009). Speciation in the Deep Sea : Multi-Locus Analysis of Divergence and Gene Flow between Two Hybridizing Species of Hydrothermal Vent Mussels. *PLOS ONE*, *4*(8), e6485. https://doi.org/10.1371/journal.pone.0006485

Gagnaire, P.-A. (2020). Comparative genomics approach to evolutionary process connectivity. *Evolutionary Applications*, *13*(6), 1320-1334. https://doi.org/10.1111/eva.12978

Gena, K. (2013). Deep Sea Mining of Submarine Hydrothermal Deposits and its Possible Environmental Impact in Manus Basin, Papua New Guinea. *Procedia Earth and Planetary Science*, *6*, 226-233. https://doi.org/10.1016/j.proeps.2013.01.031

Gutenkunst, R. N., Hernandez, R. D., Williamson, S. H., & Bustamante, C. D. (2009). Inferring the Joint Demographic History of Multiple Populations from Multidimensional SNP Frequency Data. *PLOS Genetics*, *5*(10), e1000695. https://doi.org/10.1371/journal.pgen.1000695

Hadley Wickham. (2016). *Ggplot2* (Springer-Verlag New York). https://ggplot2.tidyverse.org

Hamilton, W. D., & May, R. M. (1977). Dispersal in stable habitats. *Nature*, *269*(5629), 578-581. https://doi.org/10.1038/269578a0

Hickerson, M. J., Carstens, B. C., Cavender-Bares, J., Crandall, K. A., Graham, C. H., Johnson, J. B., Rissler, L., Victoriano, P. F., & Yoder, A. D. (2010). Phylogeography's past, present, and future : 10 years after Avise, 2000. *Molecular Phylogenetics and Evolution*, *54*(1), 291-301. https://doi.org/10.1016/j.ympev.2009.09.016

Hourdez, S., & Jollivet, D. (2019). *CHUBACARC Cruise Report*. https://doi.org/10.17600/18001111

Hourdez, S., & Jollivet, D. (2020). Chapter 2. In *Metazoan adaptation to deep-sea hydrothermal vents* (G. di Prisco, A. Huiskes and C. Ellis-Evanz (eds.), p. 42-67). Ecological reviews, Cambridge Univ. Press. https://books.google.com/books?hl=en&lr=&id=YtX7DwAAQBAJ&oi=fnd&pg=PA42&dq=info:isvZ-xX6CFwJ:scholar.google.com&ots=Iv3McwTtw5&sig=3I841J3xRdhy_EzuiOlrPwbZgSA

Hurtado, L. A., Lutz, R. A., & Vrijenhoek, R. C. (2004). Distinct patterns of genetic differentiation among annelids of eastern Pacific hydrothermal vents. *Molecular Ecology*, *13*(9), 2603-2615. https://doi.org/10.1111/j.1365-294X.2004.02287.x

Johnson, S. B., Won, Y.-J., Harvey, J. B., & Vrijenhoek, R. C. (2013). A hybrid zone between Bathymodiolus mussel lineages from eastern Pacific hydrothermal vents. *BMC Evolutionary Biology*, *13*(1), 21. https://doi.org/10.1186/1471-2148-13-21

Johnson, S. B., Young, C. R., Jones, W. J., Warén, A., & Vrijenhoek, R. C. (2006). Migration, Isolation, and Speciation of Hydrothermal Vent Limpets (*Gastropoda; Lepetodrilidae*) Across the Blanco Transform Fault. *The Biological Bulletin*, *210*(2), 140-157. https://doi.org/10.2307/4134603

Keenan, K., McGinnity, P., Cross, T. F., Crozier, W. W., & Prodöhl, P. A. (2013). diveRsity : An R package for the estimation and exploration of population genetics parameters and their associated errors. *Methods in Ecology and Evolution*, *4*(8), 782-788. https://doi.org/10.1111/2041-210X.12067

Kim, M., Kang, J.-H., and Kim, D. (2022). Holoplanktonic and meroplanktonic larvae in the surface waters of the Onnuri vent field in the Central Indian Ridge. Journal of Marine Science and Engineering, 10(2), 158. https://doi.org/10.3390/jmse10020158

Lee, W.-K., Kim, S.-J., Hou, B. K., Dover, C. L. V., & Ju, S.-J. (2019). Population genetic differentiation of the hydrothermal vent crab *Austinograea alayseae* (*Crustacea : Bythograeidae*) in the Southwest Pacific Ocean. *PLOS ONE*, *14*(4), e0215829. https://doi.org/10.1371/journal.pone.0215829

Levin, L. A. (1990). A review of methods for labeling and tracking marine invertebrate larvae. *Ophelia*, *32*(1-2), 115-144. https://doi.org/10.1080/00785236.1990.10422028

Lowe, W. H., & Allendorf, F. W. (2010). What can genetics tell us about population connectivity? *Molecular Ecology*, *19*(15), 3038-3051. https://doi.org/10.1111/j.1365-294X.2010.04688.x

Lutz, R. A., Shank, T. M., Fornari, D. J., Haymon, R. M., Lilley, M. D., Von Damm, K. L., & Desbruyeres, D. (1994). Rapid growth at deep-sea vents. *Nature*, *371*(6499), 663-664. https://doi.org/10.1038/371663a0

Mastretta-Yanes, A., Arrigo, N., Alvarez, N., Jorgensen, T. H., Piñero, D., & Emerson, B. C. (2015). Restriction site-associated DNA sequencing, genotyping error estimation and de novo assembly optimization for population genetic inference. *Molecular Ecology Resources*, *15*(1), 28-41. https://doi.org/10.1111/1755-0998.12291

Matabos, M., & Jollivet, D. (2019). Revisiting the *Lepetodrilus elevatus* species complex (*Vetigastropoda : Lepetodrilidae*), using samples from the Galápagos and Guaymas hydrothermal vent systems. *Journal of Molluscan Studies*, *85*(1), 154-165. https://doi.org/10.1093/mollus/eyy061

Matabos, M., Plouviez, S., Hourdez, S., Desbruyères, D., Legendre, P., Warén, A., Jollivet, D., & Thiébaut, E. (2011). Faunal changes and geographic crypticism indicate the occurrence of a biogeographic transition zone along the southern East Pacific Rise. *Journal of Biogeography*, *38*(3), 575-594. https://doi.org/10.1111/j.1365-2699.2010.02418.x

Matute, D. R., Butler, I. A., Turissini, D. A., & Coyne, J. A. (2010). A Test of the Snowball Theory for the Rate of Evolution of Hybrid Incompatibilities. *Science*, *329*(5998), 1518-1521. https://doi.org/10.1126/science.1193440

McPeek, M. A., & Holt, R. D. (1992). The Evolution of Dispersal in Spatially and Temporally Varying Environments. *The American Naturalist*, *140*(6), 1010-1027. https://doi.org/10.1086/285453

Mitarai, S., Watanabe, H., Nakajima, Y., Shchepetkin, A. F., & McWilliams, J. C. (2016). Quantifying dispersal from hydrothermal vent fields in the western Pacific Ocean. *Proceedings of the National Academy of Sciences*, *113*(11), 2976-2981. https://doi.org/10.1073/pnas.1518395113

Moalic, Y., Desbruyères, D., Duarte, C. M., Rozenfeld, A. F., Bachraty, C., & Arnaud-Haond, S. (2012). Biogeography Revisited with Network Theory : Retracing the History of Hydrothermal Vent Communities. *Systematic Biology*, *61*(1), 127-127. https://doi.org/10.1093/sysbio/syr088

Mouchi, V., Pecheyran, C., Claverie, F., Cathalot, C., Matabos, M., Germain, Y., Rouxel, O., Jollivet, D., Broquet, T., & Comtet, T. (2024). A step towards measuring connectivity in the deep sea : Elemental fingerprints of mollusk larval shells discriminate hydrothermal-vent sites. *Biogeosciences*, *21*(1), 145-160. https://doi.org/10.5194/bg-21-145-2024

Nei, M., & Li, W. H. (1979). Mathematical model for studying genetic variation in terms of restriction endonucleases. *Proceedings of the National Academy of Sciences*, *76*(10), 5269-5273. https://doi.org/10.1073/pnas.76.10.5269

Niner, H. J., Ardron, J. A., Escobar, E. G., Gianni, M., Jaeckel, A., Jones, D. O. B., Levin, L. A., Smith, C. R., Thiele, T., Turner, P. J., Van Dover, C. L., Watling, L., & Gjerde, K. M. (2018). Deep-Sea Mining With No Net Loss of Biodiversity—An Impossible Aim. *Frontiers in Marine Science*, *5*. https://www.frontiersin.org/article/10.3389/fmars.2018.00053

Papadopoulou, A., & Knowles, L. L. (2016). Toward a paradigm shift in comparative phylogeography driven by trait-based hypotheses. *Proceedings of the National Academy of Sciences*, *113*(29), 8018-8024. https://doi.org/10.1073/pnas.1601069113

Paris, J. R., Stevens, J. R., & Catchen, J. M. (2017). Lost in parameter space : A road map for stacks. *Methods in Ecology and Evolution*, *8*(10), 1360-1373. https://doi.org/10.1111/2041-210X.12775

Pickrell, J. K., & Pritchard, J. K. (2012). Inference of Population Splits and Mixtures from Genome-Wide Allele Frequency Data. *PLOS Genetics*, *8*(11), e1002967. https://doi.org/10.1371/journal.pgen.1002967

Plouviez, S., Faure, B., Guen, D. L., Lallier, F. H., Bierne, N., & Jollivet, D. (2013). A new barrier to dispersal trapped old genetic clines that escaped the easter microplate tension zone of the Pacific vent mussels. *PLOS ONE*, *8*(12), e81555. https://doi.org/10.1371/journal.pone.0081555

Plouviez, S., LaBella, A. L., Weisrock, D. W., Meijenfeldt, F. A. B. von, Ball, B., Neigel, J. E., & Dover, C. L. V. (2019). Amplicon sequencing of 42 nuclear loci supports directional gene flow between South Pacific populations of a hydrothermal vent limpet. *Ecology and Evolution*, *9*(11), 6568-6580. https://doi.org/10.1002/ece3.5235

Plouviez, S., Le Guen, D., Lecompte, O., Lallier, F. H., & Jollivet, D. (2010). Determining gene flow and the influence of selection across the equatorial barrier of the East Pacific Rise in the tube-dwelling polychaete *Alvinella pompejana*. *BMC Evolutionary Biology*, *10*(1), 220. https://doi.org/10.1186/1471-2148-10-220

Plouviez, S., Shank, T. M., Faure, B., Daguin-Thiebaut, C., Viard, F., Lallier, F. H., & Jollivet, D. (2009). Comparative phylogeography among hydrothermal vent species along the East Pacific Rise reveals vicariant processes and population expansion in the South. *Molecular Ecology*, *18*(18), 3903-3917. https://doi.org/10.1111/j.1365-294X.2009.04325.x

Poitrimol, C., Thiébaut, É., Daguin-Thiébaut, C., Port, A.-S. L., Ballenghien, M., Y, A. T. L., Jollivet, D., Hourdez, S., & Matabos, M. (2022). Contrasted phylogeographic patterns of hydrothermal vent gastropods along South West Pacific : Woodlark Basin, a possible contact zone and/or stepping-stone. *PLOS ONE*, *17*(10), e0275638. https://doi.org/10.1371/journal.pone.0275638

Poitrimol, C., Matabos, M., Veuillot, A., Ramière, A., Comtet, T., Boulart, C., Cathalot, C., & Thiébaut, É. (2024). Reproductive biology and population structure of three hydrothermal gastropods (*Lepetodrilus schrolli, L. fijiensis* and *Shinkailepas tollmanni*) from the South West Pacific back-arc basins. *Marine Biology*, *171*(1), 31. https://doi.org/10.1007/s00227-023-04348-4

R Core Team. (2023). https://www.R-project.org/

Ravinet, M., Faria, R., Butlin, R. K., Galindo, J., Bierne, N., Rafajlović, M., Noor, M. a. F., Mehlig, B., & Westram, A. M. (2017). Interpreting the genomic landscape of speciation : A road map for finding barriers to gene flow. *Journal of Evolutionary Biology*, *30*(8), 1450-1477. https://doi.org/10.1111/jeb.13047

Rochette, N. C., Rivera-Colón, A. G., & Catchen, J. M. (2019). Stacks 2 : Analytical methods for paired-end sequencing improve RADseq-based population genomics. *Molecular Ecology*, *28*(21), 4737-4754. https://doi.org/10.1111/mec.15253

Rougeux, C., Bernatchez, L., & Gagnaire, P.-A. (2017). Modeling the Multiple Facets of Speciation-with-Gene-Flow toward Inferring the Divergence History of Lake Whitefish Species Pairs (*Coregonus clupeaformis*). *Genome Biology and Evolution*, *9*(8), 2057-2074. https://doi.org/10.1093/gbe/evx150

Schellart, W. P., Lister, G. S., & Toy, V. G. (2006). A Late Cretaceous and Cenozoic reconstruction of the Southwest Pacific region : Tectonics controlled by subduction and slab rollback processes. *Earth-Science Reviews*, *76*(3), 191-233. https://doi.org/10.1016/j.earscirev.2006.01.002

Schöne, B. R., & Giere, O. (2005). Growth increments and stable isotope variation in shells of the deep-sea hydrothermal vent bivalve mollusk *Bathymodiolus brevior* from the North Fiji

Basin, Pacific Ocean. *Deep Sea Research Part I: Oceanographic Research Papers*, *52*(10), 1896-1910. https://doi.org/10.1016/j.dsr.2005.06.003

Shank, T. M., Fornari, D. J., Von Damm, K. L., Lilley, M. D., Haymon, R. M., & Lutz, R. A. (1998). Temporal and spatial patterns of biological community development at nascent deep-sea hydrothermal vents (9°50'N, East Pacific Rise). *Deep Sea Research Part II: Topical Studies in Oceanography*, *45*(1), 465-515. https://doi.org/10.1016/S0967-0645(97)00089-1

Sommer, S. A., Van Woudenberg, L., Lenz, P. H., Cepeda, G., & Goetze, E. (2017). Vertical gradients in species richness and community composition across the twilight zone in the North Pacific Subtropical Gyre. *Molecular Ecology*, *26*(21), 6136-6156. https://doi.org/10.1111/mec.14286

Sundqvist, L., Keenan, K., Zackrisson, M., Prodöhl, P., & Kleinhans, D. (2016). Directional genetic differentiation and relative migration. *Ecology and Evolution*, *6*(11), 3461-3475. https://doi.org/10.1002/ece3.2096

Teixeira, S., Serrão, E. A., & Arnaud-Haond, S. (2012). Panmixia in a Fragmented and Unstable Environment : The Hydrothermal Shrimp *Rimicaris exoculata* Disperses Extensively along the Mid-Atlantic Ridge. *PLOS ONE*, *7*(6), e38521. https://doi.org/10.1371/journal.pone.0038521

Thaler, A. D., Plouviez, S., Saleu, W., Alei, F., Jacobson, A., Boyle, E. A., Schultz, T. F., Carlsson, J., & Dover, C. L. V. (2014). Comparative Population Structure of Two Deep-Sea Hydrothermal-Vent-Associated Decapods (*Chorocaris sp. 2* and *Munidopsis lauensis*) from Southwestern Pacific Back-Arc Basins. *PLOS ONE*, *9*(7), e101345. https://doi.org/10.1371/journal.pone.0101345

Thaler, A. D., Zelnio, K., Saleu, W., Schultz, T. F., Carlsson, J., Cunningham, C., Vrijenhoek, R. C., & Van Dover, C. L. (2011). The spatial scale of genetic subdivision in populations of *Ifremeria nautilei,* a hydrothermal-vent gastropod from the southwest Pacific. *BMC Evolutionary Biology*, *11*(1), 372. https://doi.org/10.1186/1471-2148-11-372

Tran Lu Y, A., Ruault, S., Daguin-Thiébaut, C., Castel, J., Bierne, N., Broquet, T., Wincker, P., Perdereau, A., Arnaud-Haond, S., Gagnaire, P.-A., Jollivet, D., Hourdez, S., & Bonhomme, F. (2022). Subtle limits to connectivity revealed by outlier loci within two divergent

metapopulations of the deep-sea hydrothermal gastropod *Ifremeria nautilei*. *Molecular Ecology*, *31*(10), 2796-2813. https://doi.org/10.1111/mec.16430

Tunnicliffe, V. (1992). The Nature and Origin of the Modern Hydrothermal Vent Fauna. *PALAIOS*, *7*(4), 338-350. https://doi.org/10.2307/3514820

Tunnicliffe, V., Chen, C., Giguère, T., Rowden, A. A., Watanabe, H. K., & Brunner, O. (2024). Hydrothermal vent fauna of the western Pacific Ocean : Distribution patterns and biogeographic networks. *Diversity and Distributions*, *30*(2), e13794. https://doi.org/10.1111/ddi.13794

Van Dover, C. L. (2011). Mining seafloor massive sulphides and biodiversity : What is at risk? *ICES Journal of Marine Science*, *68*(2), 341-348. https://doi.org/10.1093/icesjms/fsq086

Van Dover, C. L., Ardron, J. A., Escobar, E., Gianni, M., Gjerde, K. M., Jaeckel, A., Jones, D. O. B., Levin, L. A., Niner, H. J., Pendleton, L., Smith, C. R., Thiele, T., Turner, P. J., Watling, L., & Weaver, P. P. E. (2017). Biodiversity loss from deep-sea mining. *Nature Geoscience*, *10*(7), Article 7. https://doi.org/10.1038/ngeo2983

Vrijenhoek, R. C. (2010). Genetic diversity and connectivity of deep-sea hydrothermal vent metapopulations. *Molecular Ecology*, *19*(20), 4391-4411. https://doi.org/10.1111/j.1365-294X.2010.04789.x

Waples, R. S., & Gaggiotti, O. (2006). INVITED REVIEW : What is a population? An empirical evaluation of some genetic methods for identifying the number of gene pools and their degree of connectivity. *Molecular Ecology*, *15*(6), 1419-1439. https://doi.org/10.1111/j.1365-294X.2006.02890.x

Warèn, A., & Bouchet, P. (1993). New records, species, genera, and a new family of gastropods from hydrothermal vents and hydrocarbon seeps*. *Zoologica Scripta*, *22*(1), 1-90. https://doi.org/10.1111/j.1463-6409.1993.tb00342.x

Washburn, T. W., Turner, P. J., Durden, J. M., Jones, D. O. B., Weaver, P., & Van Dover, C. L. (2019). Ecological risk assessment for deep-sea mining. *Ocean & Coastal Management*, *176*, 24-39. https://doi.org/10.1016/j.ocecoaman.2019.04.014

Yahagi, T., Fukumori, H., Warén, A., & Kano, Y. (2019). Population connectivity of hydrothermal-vent limpets along the northern Mid-Atlantic Ridge (*Gastropoda : Neritimorpha: Phenacolepadidae*). *Journal of the Marine Biological Association of the United Kingdom*, *99*(1), 179-185. https://doi.org/10.1017/S0025315417001898

Yahagi, T., Thaler, A. D., Dover, C. L. V., & Kano, Y. (2020). Population connectivity of the hydrothermal-vent limpet *Shinkailepas tollmanni* in the Southwest Pacific (*Gastropoda : Neritimorpha: Phenacolepadidae*). *PLoS One*, *15*(9), e0239784. https://doi.org/10.1371/journal.pone.0239784

Young, C. M. (1994). A tale of two dogmas: the early history of deep-sea reproductive biology. *Reproduction, larval biology, and recruitment in the deep-sea benthos. Columbia University Press, New York*, 1-25.

Zheng, X., Levine, D., Shen, J., Gogarten, S. M., Laurie, C., & Weir, B. S. (2012). A high-performance computing toolset for relatedness and principal component analysis of SNP data. *Bioinformatics*, *28*(24), 3326-3328. https://doi.org/10.1093/bioinformatics/bts606